deleting amino acid residues 115 to 149 in the V1 loop, 153 to 209 in the V2 loop, 313 to 342 in the V3 loop, and 404 to 430 in the V4 loop and replacing them with Gly-Ala-Gly, Gly, Gly-Ala, and Gly-Ala-Gly, respectively. These mutations were introduced into RE543-EGFP using primers DV1F (5′-ATG TAA TGG AGC CGG CTC TTG CAT AAA AAA-3′) and DV1R (5′-AAG AGC CGG CTC CAT TAC ATC TCA TTG CTA-3′) for ΔV1, DV2F (5′-ATA GGA GCC GGC CAT TGT AAC ACC AGT-3′) and DV2R (5′-ACA ATG GCC GGC TCC TAT GCA AGA ATC ACC-3′) for ΔV2, DV3F (5′-TGT AGA GGA GCC GGC TGG TGC CGG TTT GGA-3′) and DV3R (5′-GCA CCA GCC GGC TCC TCT ACA TTT CAT TGT-3′) for ΔV3, and DV4F (5′-AAG AAT TCT TAT ACT GCA AAG GAG CCG GCC CAT GTC ATA TTA GAC AAA-3′) for ΔV4. Mutant ΔGly was constructed using primers N306AFw2 (5′-TAT TAT GCT CTA ACA ATG AAA TGT AG-3′), N306ARv (5′-CAT TGT TAG AGC ATA ATA CTT-3′), N316AFw (5′-AGA CCA GGA GCT AAG ACA GTT-3′), N316ARv (5′-AAC TGT CTT AGC TCC TGG TCT-3′), N349AFw (5′-GGT TTG GAG GAG CCT GGA GCG-3′), and N349ARv (5′-CGC TCC AGG CTC CTC CAA ACC G-3′) to introduce the mutations N306A, N316A, and N349A at potential N-linked glycosylation sites. Mutant D385R was constructed using primers S-D368RFw (5′-CCA GCA GGA GGA CGT CCA GAA GTC AC-3′) and S-D368RRv (5′-TTC TGG ACG TCC TCC TGC TGG AGC TGT-3′). The D385R substitution in SIVsmE543-3 corresponds to D368R in HIV-1, which interferes with CD4 binding site (CD4bs) antibodies (13, 44, 45). Mutant I434R was constructed using primers S-I420RFw (5′-GCC ATG TCA TCG TAG ACA AAT AAT CAA C −3′) and S-I420RRv (5′-GAT TAT TTG TCT ACG ATG ACA TGG CAC −3′). The I434R substitution in SIVsmE543-3 corresponds to I420R in HIV-1, which interferes with CD4-induced (CD4i) antibodies (13, 45, 46). Amino acid numbering of Env was based on that of SIVmac239, the reference sequence of SIV, and the HIV-2 sequence in the Los Alamos HIV databases (http://www.hiv.lanl.gov/).

**Flow-cytometric analysis.** Plasmids to express wild-type and mutant Env were transfected into 293T cells using X-tremeGENE 9 DNA transfection reagent (Roche Molecular Biochemicals) according to the manufacturer's instructions. After incubation for 2 days, the transfected cells were detached with PBS containing 0.05% trypsin and 0.53 mM EDTA and adjusted to $1 \times 10^7$ cells/ml in PBS containing 0.2% bovine serum albumin (BSA). To examine the reactivity of Fab, we incubated 50 μl cells with 10 μl 50 ng/μl Fab for 40 min at RT. After washing with PBS containing 0.2% BSA, the cells were incubated with 50 μl anti-HA antibody (1:200; 3F10; Roche Molecular Biochemicals) for 20 min at RT, followed by incubation with 50 μl allophycocyanin (APC)-conjugated AffiniPure goat anti-rat IgG (H+L) $F(ab')_2$ fragment (1:200; Jackson ImmunoResearch Laboratories, Inc., West Grove, PA) for 20 min at RT. When enhancement with sCD4 was examined, cells were resuspended in PBS containing 0.2% BSA in the presence or absence of 2 μg/ml sCD4 at $1 \times 10^7$ cells/ml before staining. After incubation with sCD4 for 15 min at RT, 20 μl of cells was mixed with 10 μl 25 ng/μl Fab and stained with anti-HA and anti-rat antibodies. Murine MAb KK46 (1:200) was used as a control antibody against the linear V3 epitope (47). KK46-incubated cells were stained by APC-conjugated goat anti-mouse Ig (1:200; BD Biosciences, Franklin Lakes, NJ). The stained cells were analyzed using a FACSCalibur flow cytometer (BD Biosciences). The reactivity of Fab to Env was determined by comparison with an unstained control after gating $EGFP^+$ cells. Data analysis was performed using FlowJo (TreeStar, San Carlos, CA).

**Isolation of B404-resistant variants from SIVmac316.** The selection of B404-resistant variants from SIVmac316 was performed as described previously (48, 49). Briefly, 5,000 $TCID_{50}$ SIVmac316 was incubated with 5 ng/ml Fab B404 for 30 min at 37°C. Then, $5 \times 10^4$ PM1/CCR5 cells were added to the virus-Fab mixture. After incubation for 5 h, cells were washed with PBS and resuspended in RPMI 1640 medium supplemented with 10% FBS without Fab B404. The culture supernatant was harvested on day 7 and used to infect fresh PM1/CCR5 cells for the next round of culture in the presence of increasing concentrations of Fab B404. A B404-resistant virus, P26B404, was recovered from the cell culture supernatant at passage 26 at 400 μg/ml Fab B404. SIVmac316 was also passaged for the same period in PM1/CCR5 cells in the absence of Fab B404, and the resulting virus was designated P26C. Proviral DNA samples were extracted from PM1/CCR5 cells infected with P26B404 and P26C using a QIAamp DNA blood minikit (Qiagen). The gp120 region was amplified by PCR using primers SEnv-F (5′-ATG GGA TGT CTT GGG AAT CAG C-3′) and SER1 (5′-CCA AGA ACC CTA GCA CAA AGA CCC-3′), cloned using a TA cloning kit (Invitrogen), and subjected to sequencing.

**Nucleic acid sequence analysis.** The Ig variable regions were sequenced using the primers ompseq and pelseq (40), and analyzed with V-QUEST in the International Immunogenetics Database (IMGT; http://www.imgt.org/) (50). The germ line sequence of the VH gene, from which B404 originated, was determined using the genome database of rhesus macaque (51). Sequences were aligned and phylogenetically analyzed using Molecular Evolutionary Genetics Analysis version 5 (MEGA5) (52).

The gp120 region from P26B404 and P26C was sequenced using primers M13F and M13R in the vector and SE1 (5′-ATA ATA CAG TCA CAG AAC A-3′). Predicted amino acid sequences were aligned using CLC Sequence Viewer 6 (CLC Bio, Aarhus, Denmark), together with other SIV sequences.

**Molecular dynamics (MD) simulation of gp120 from B404-resistant variants.** MD simulations of the gp120 outer domain of SIVmac316 and the mutants with a F277V or N295S substitution were performed essentially as described for MD simulations of the HIV-1 gp120 outer domain (53). SIV gp120 outer domain structures with various V3 regions were constructed using the homology modeling technique with the Molecular Operating Environment (MOE) 2011.10 (Chemical Computing Group Inc., Montreal, Quebec, Canada). The modeling template was the crystal structure of HIV-1 gp120 containing the entire V3 region at a resolution of 3.30 Å (PDB code, 2QAD [54]) and the SIV gp120 core at a resolution of 4.00 Å (PDB code, 3FUS [55]). The 195 amino-terminal and 7 carboxyl-terminal residues were deleted to construct the gp120 outer domain structures. Glycans were added to the gp120 outer domain structures using Online Glycoprotein Builder (56). MD simulations were performed using the SANDER module in the AMBER 10 program package (57, 58) and the AMBER force field (59) and GLYCAM06 (60) with the TIP3P water model (61). Bond lengths involving hydrogen were constrained with SHAKE (62), and the time step for all MD simulations was set to 2 fs. A nonbonded cutoff of 12 Å was used. After heating calculations for 20 ps until 310 K using the NVT ensemble, the simulations were executed using the NPT ensemble at 1 atm and at 310 K for 50 ns. To map structurally fluctuating sites in the gp120 outer domain, we calculated the root mean square fluctuation (RMSF) of the main chains of individual amino acid residues as described previously (53). Briefly, the RMSF were calculated using the 90,000 snapshots obtained from MD simulations of 5 to 50 ns. The average structures during these MD simulations were used as reference structures for the calculation of the RMSF using the ptraj module in AMBER 10.

**Nucleotide sequence accession numbers.** Sequence data for Ig clones obtained from SIVsmH635FC-infected macaques were submitted to GenBank under accession numbers JF925337 to JF925378 and JF925380 to JF926116.

## RESULTS

**Potent and broad neutralizing activity of NAb B404 against various SIV strains.** SIV-specific Fab clones were previously isolated from the Fab library from SIVsmH635FC-infected macaque H723 through panning against whole SIV Ag (25). Four Fab clones specific to gp120, represented by B404, showed similar gene usage, epitope specificity, and neutralizing activity that covered homologous and heterologous SIV strains. To define the neutralizing potency of B404 further, IgG, Fab, and scFv with B404 variable regions were constructed and examined for their neutralizing ac-

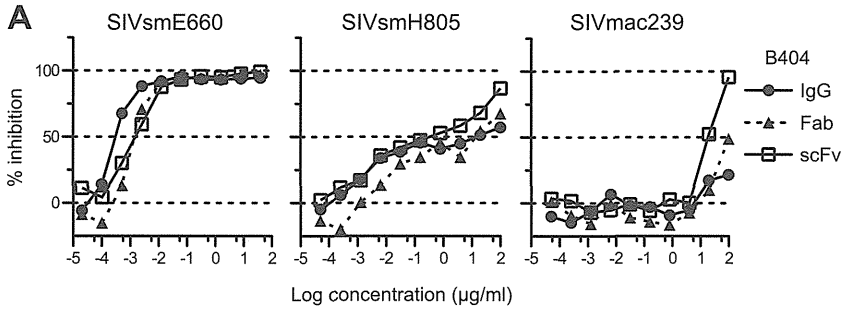


B

$IC_{50}$ and $IC_{90}$(μg/ml) of IgG, Fab and scFv of B404 against various SIV strains.

| Virus | % aa difference | IgG | | Fab | | scFv | |
|---|---|---|---|---|---|---|---|
| | | IC50 | IC90 | IC50 | IC90 | IC50 | IC90 |
| SIVmac316 | 16.8 | 2.5E-04 | 1.9E-03 | 6.0E-04 | 4.8E-03 | 4.5E-04 | 1.9E-03 |
| SIVsmE660 | 7.3 | 3.0E-04 | 2.5E-03 | 1.4E-03 | 7.8E-03 | 1.6E-03 | 2.0E-02 |
| SIVsmH635FC | 0 | 1.6E-03 | 5.8E-03 | 3.7E-03 | 1.4E-02 | 2.1E-03 | 1.0E-02 |
| SIVsmE543-3 | 1.1 | 2.4E-03 | >100 | 2.7E-03 | >100 | 2.6E-03 | 80 |
| SIVsmH805 | 7.5 | 16 | >100 | 5.0 | >100 | 5.2E-01 | >100 |
| SIVsmH807 | 6.9 | >100 | >100 | 9.1 | >100 | 2.8 | >100 |
| SIVmac239 | 16.4 | >100 | >100 | >100 | >100 | 19 | 51 |
| HIV-$2_{GH123}$ | 29.3 | >100 | >100 | >100 | >100 | >100 | >100 |
| HIV-$1_{NL432}$ | 59.7 | >100 | >100 | >100 | >100 | >100 | >100 |

< 1.0E-02 | 1.0E-02 - 1.0E+00 | 1 - 100 | > 100 μg/ml

**FIG 1** Potent and broad neutralization by monoclonal antibody B404 from a SIVsmH635FC-infected macaque. (A) The neutralizing potencies of IgG, Fab, and scFv of B404 are shown by inhibition kinetics against SIVsmE660FL14, SIVsmH805-24w-3, and SIVmac239. (B) The neutralizing potencies of IgG, Fab and scFv of B404 are shown by $IC_{50}$ and $IC_{90}$ (μg/ml). Seven SIV strains, HIV-$2_{GH123}$ and HIV-$1_{NL432}$ were examined for their neutralizing sensitivities against B404 in TZM-bl cells. The $IC_{50}$ and $IC_{90}$ values are shown in dark gray ($<1.0 \times 10^{-2}$ μg/ml), medium gray ($1.0 \times 10^{-2}$ to $1.0 \times 10^{0}$ μg/ml), light gray (1 to 100 μg/ml) and white (>100 μg/ml). Percent amino acid differences were calculated by pairwise comparison with SIVsmH635FC.

tivity against 7 SIV strains (Fig. 1). These SIV strains were classified into 2 lineages, lineage 1 (SIVsmE660, SIVsmH635FC, SIVsmE543-3, SIVsmH805, and SIVsmH807) and lineage 8 (SIVmac316 and SIVmac239), according to the phylogenetic analysis by Apetrei et al. (63), which identified nine divergent lineages in SIVsm/mac corresponding to HIV-1 subtypes. Sensitivity to neutralization was known to be high in SIVmac316, SIVsmE660, and SIVsmH635FC (25, 38). Infection with these neutralization-sensitive SIV strains was almost completely blocked by low concentrations of all forms of B404. Although the potency to inhibit infection was similar among IgG, Fab, and scFv, B404 IgG was slightly more effective against these SIV strains, as shown by the neutralizing kinetics of SIVsmE660 (Fig. 1A). Neutralization of SIVsmE543-3, SIVsmH805, and SIVsmH807 reached a plateau at 10 to 100 ng/ml IgG B404 and Fab B404, as represented by neutralization kinetics against SIVsmH805 (Fig. 1A). These viruses were moderately sensitive to B404-mediated neutralization, although the $IC_{50}$s were variable among these SIV strains (Fig. 1B). Interestingly, B404 scFv was more effective at high concentrations than B404 IgG and B404 Fab in neutralization of these moderately neutralization-sensitive viruses and SIVmac239, which is a highly neutralization-resistant strain (Fig. 1). Infection with SIVmac239 was unaffected by the presence of any form of B404 at a concentration of less than 1 μg/ml but was inhibited more than 90% by 100 μg/ml B404 scFv. Neutralization of 7 of 7 SIV strains, including genetically diverse, neutralization-resistant SIVmac239, by B404 scFv indicates that B404 is a potent and broad NAb against SIVsm/mac strains.

**Isolation of Env-specific Fab clones from SIVsmH635FC-infected macaques.** To analyze the induction of B404-like antibodies in SIV-infected macaques, Env-specific Fab clones were isolated from 4 SIVsmH635FC-infected macaques: H723, H704, H709, and H714 (26, 39). Env-specific Fab clones from H723 were isolated from the previously constructed phage library (25) through panning against Env, which was conjugated by coating plate wells with the anti-Env Fab clones B404 (anti-gp120 conformational), B408 (anti-gp41 cluster I), and H301 (anti-gp120 V1). Together with anti-Env Fab clones from the previous study, 98 anti-Env Fab clones, including 33 NAbs (33.7%), were obtained from H723. From 3 other SIVsmH635FC-infected macaques, κ and λ light-chain phage libraries were separately constructed, and 2 panning series were performed using B404 and H301 to conjugate Env. After 4 series of panning in each macaque, we obtained 155, 102, and 53 independent Fab clones from H704, H709, and

TABLE 1 Preferential gene usage and competition with B404 of NAbs

| Inoculated virus | Animal | Frequency (%) of NAbs[a] | No. of NAbs | % of NAbs with: | | Avg CDRH3 length[b] | Competition (%) with B404[c] |
|---|---|---|---|---|---|---|---|
| | | | | VH3 genes | λ light chains | | |
| SIVsmH635FC | H723 | 33.7 | 33 | 81.8 | 93.9 | 20.0 | 81.8 |
| | H704 | 30.3 | 47 | 95.7 | 97.9 | 18.7 | 100 |
| | H709 | 7.8 | 8 | 75.0 | 100 | 17.8 | 100 |
| | H714 | 52.8 | 28 | 96.4 | 92.9 | 18.7 | 100 |
| SIV mix[d] | H711 | 17.2 | 15 | 26.7 | 40.0 | 15.2 | 86.7 |
| | H725 | 2.2 | 1 | 0.0 | 100 | 12 | 100 |

[a] Frequencies of Fab clones with the VH3 gene and λ light chain are shown as percentages of NAbs.
[b] Average number of amino acids in CDRH3.
[c] Competition ELISA with 2 μg/ml B404 IgG was performed. The frequency of Fabs showing more than 50% inhibition is shown as a percentage of NAbs.
[d] H711 was inoculated with a mixture of SIVsmE543-3 and SIVsmH635FC. H725 was inoculated with plasma samples from 2 SIVsmH445-infected macaques, H631 and H635.

H714, respectively. Neutralizing activities were observed in 47 clones (30.3%) from H704, 9 clones (8.8%) from H709, and 28 clones (52.8%) from H714 (Table 1). Phylogenetic analysis of VH genes revealed that 105 NAbs formed a major NAb cluster with B404 (Fig. 2). The remaining NAbs were separated into 3 minor clusters containing 3 or 4 NAbs. Fab clones in the major group, designated the B404 group, were isolated from all 4 macaques analyzed.

Although Fab clones in the B404 group were genetically similar to one another, several small clusters were observed in the B404 group, suggesting multiple B cell origins generated by VDJ recombination in these B404-like NAbs. Sequence analysis using the International Immunogenetics Database (50) indicated that the VH genes of Fab clones in the B404 group were close to human pseudogene IGHV3-h (approximately 90% identity), but no functional VH gene showed >90% identity. Analysis using the genome database of the rhesus macaque (51) revealed a significant relationship (>95% identity) between Fab clones in the B404 group and the rhesus macaque VH3 gene in the chromosome 7 scaffold (GenBank accession number NW_001122023). These results suggest that a major group of NAbs in SIVsmH635FC-infected macaques preferentially use the same rhesus VH3 germ line that lacks a human counterpart.

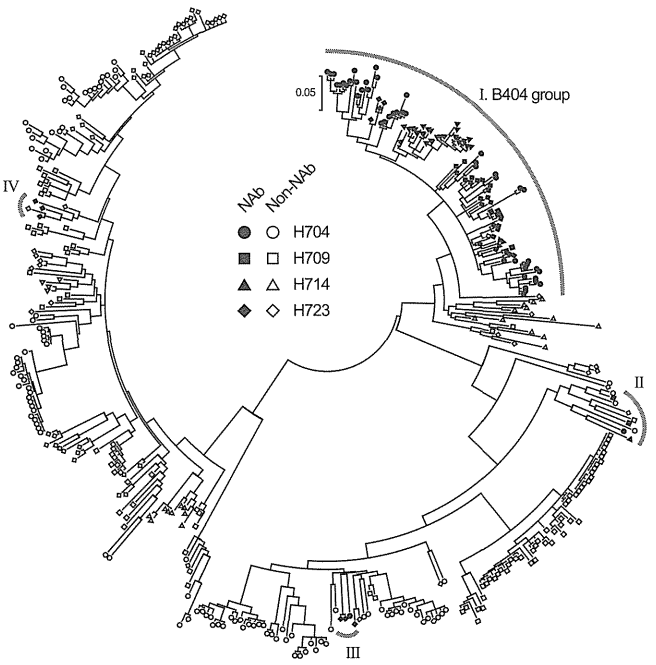


FIG 2 B404-like NAbs formed a major group in anti-Env antibodies from 4 SIVsmH635FC-infected rhesus macaques. NAbs were separated into 4 groups in the phylogenetic tree, which was generated using MEGA5 (70) from heavy-chain genes of 98, 155, 102, and 53 Fab clones from H704, H709, H714, and H723, respectively.

**Bias in gene usage of NAbs from SIVsmH635FC-infected macaques.** The genetic features of anti-Env Fab clones are summarized in Fig. 3 and Table 1. As mentioned above, a major population of NAbs from SIVsmH635FC-infected macaques used the same VH3 gene as B404, resulting in a high rate of NAbs using the VH3 gene (Fig. 3A and Table 1). A high occupancy of λ light chains was also characteristic of NAbs from SIVsmH635FC-infected macaques (Fig. 3B and Table 1). Moreover, a long complementarity-determining region 3 loop of the heavy chain (CDRH3) was characteristic of the NAbs (Fig. 3C and Table 1). CDRH3 of most NAbs had 19 or more amino acids, although the length of CDRH3 was usually less than 18 amino acids in nonneutralizing Fab clones. These results clearly showed that B404-like NAbs with the VH3 gene-encoded heavy chain with a long CDR3 and λ light chain are the main NAb population in SIVsmH635FC-infected macaques. In contrast, Fab clones from macaques H711 and H725 lacked these remarkable features of B404-like NAbs (Fig. 3, bottom; Table 1). These 2 macaques were inoculated with a mixture of SIVs (SIV mix). H711 was infected with a combination of SIVsmE543-3 and SIVsmH635FC. H725 was infected with plasma samples from 2 SIVsmH445-infected macaques, H631 and H635, which SIVsmH635FC was isolated from. Although anti-Env Fab clones were similarly isolated from these macaques, the frequency of NAbs from H711 (17.2%) and H725 (2.2%) was lower than that from SIVsmH635FC-infected macaques (8.8 to 52%). NAbs from H711 and H725 preferentially used VH1 gene-encoded heavy chains with a short CDRH3 and κ light chains, but NAbs from these macaques showed a genetic variation, similarly to those in HIV-1-infected patients (64). These results suggested that B404-like NAbs are induced exclusively in SIVsmH635FC-infected macaques.

**Potent neutralizing activity and the same specificity of NAbs in the B404 group.** To analyze the epitopes recognized by these NAbs, we first separated Fabs with neutralizing activity into 2 groups according to the results of competition ELISA with B404 IgG. All the NAbs in the B404 group and group II (Fig. 2) com-

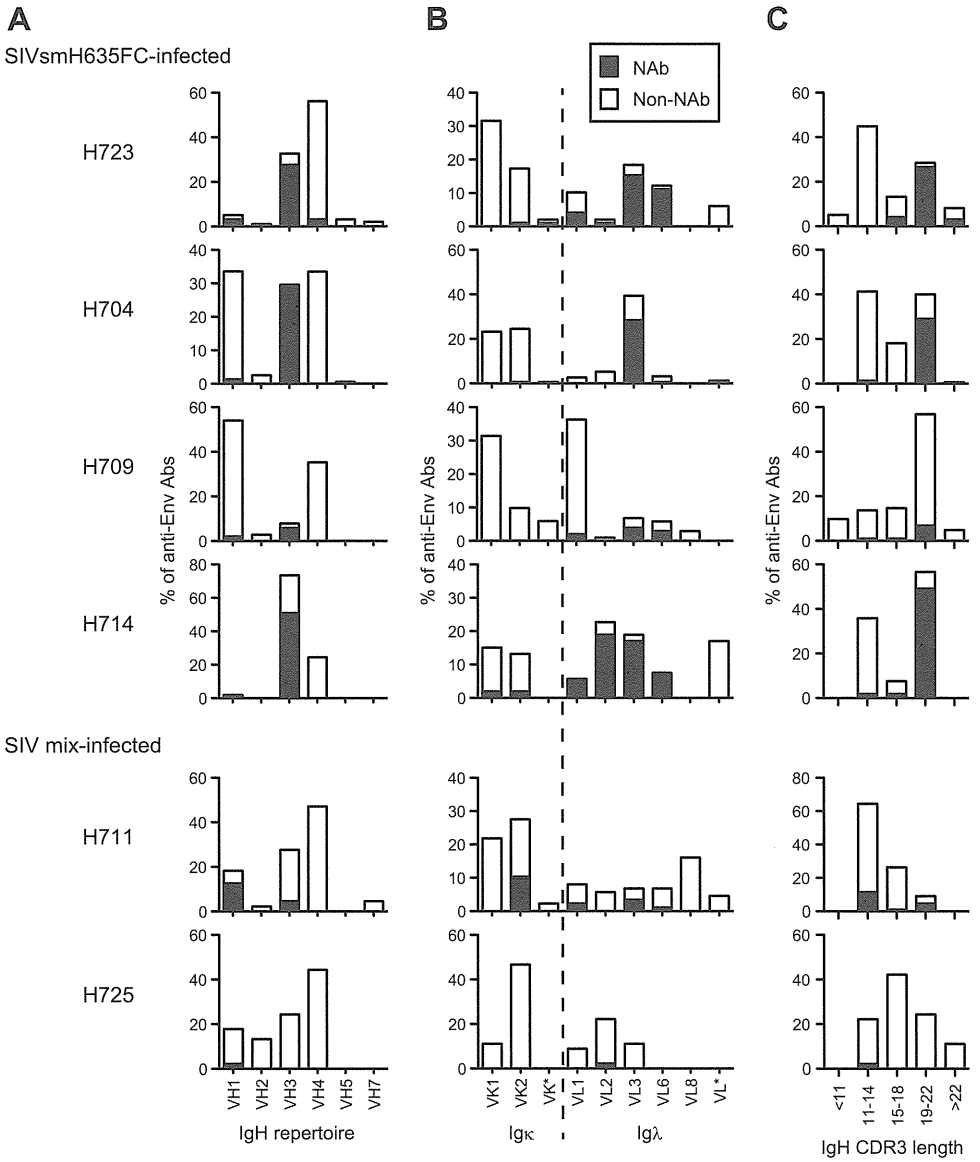


**FIG 3** Bias in the Ig gene usage and CDR3 length of neutralizing Fab clones from SIVsmH635FC-infected macaques. The proportions of IgH (A) and Igκ and Igλ (B) repertoires and heavy-chain CDR3 length (C) are shown as percentages of NAbs and non-NAbs. In addition to Fabs isolated from 4 SIVsmH635FC-infected macaques, 87 Fab clones from H711, which was infected with a combination of SIVsmE543-3 and SIVsmH635FC, and 45 Fab clones from H725, which was infected with plasma samples from 2 SIVsmH445-infected macaques, H631 and H635, were similarly analyzed. Usage of Ig genes was analyzed using V-QUEST in the International Immunogenetics Database (44).

peted with B404 IgG (Fig. 4A), suggesting that epitopes for these NAbs overlap or are close to that for B404. Despite the differences in gene usage, competition with B404 IgG was also observed in most NAbs from macaques infected with SIV mix (Table 1). NAbs belonging to groups III and IV, with the exception of 1 Fab in group III, did not compete with B404 IgG (Fig. 4A). The binding ability of these Fabs was even enhanced by the addition of B404. Competition of the Fabs in groups III and IV with biotinylated K8 in group III suggested that the Fabs in group III and IV share the same epitope (data not shown). The neutralizing activity of these Fabs was examined against the genetically divergent SIVmac316 and the neutralization-resistant SIVsmE543-3 (Fig. 4B). All of the Fabs tested showed at least 50% inhibition against both viruses, and the B404 group included Fabs with potent neutralizing activity that showed efficient inhibition at low concentrations. Accordingly, the $IC_{50}$s of the 4 Fabs in the B404 group ranged from 0.8 to 316 ng/ml (average $IC_{50}$, 79 ng/ml) against SIVmac316, indicating the presence of NAbs comparable to B404 ($IC_{50}$ against SIVmac316, 0.6 ng/ml) (Fig. 1). In contrast, $IC_{50}$ against SIVmac316 ranged between 32 and 908 ng/ml (average $IC_{50}$, 243 ng/ml) in groups III and IV. This result suggests that B404-like NAbs are the main NAb population in terms of number and neutralizing potency.

**Epitope mapping of NAb B404.** To define the region of the Env targeted by B404, we examined reactivity against mutants of SIVsmE543-3 Env. Because the V3 loop has been shown to be important for B404 binding (25), mutants with deletions in the V1, V2, V3, and V4 loops (ΔV1, ΔV2, ΔV3, and ΔV4) and a mu-

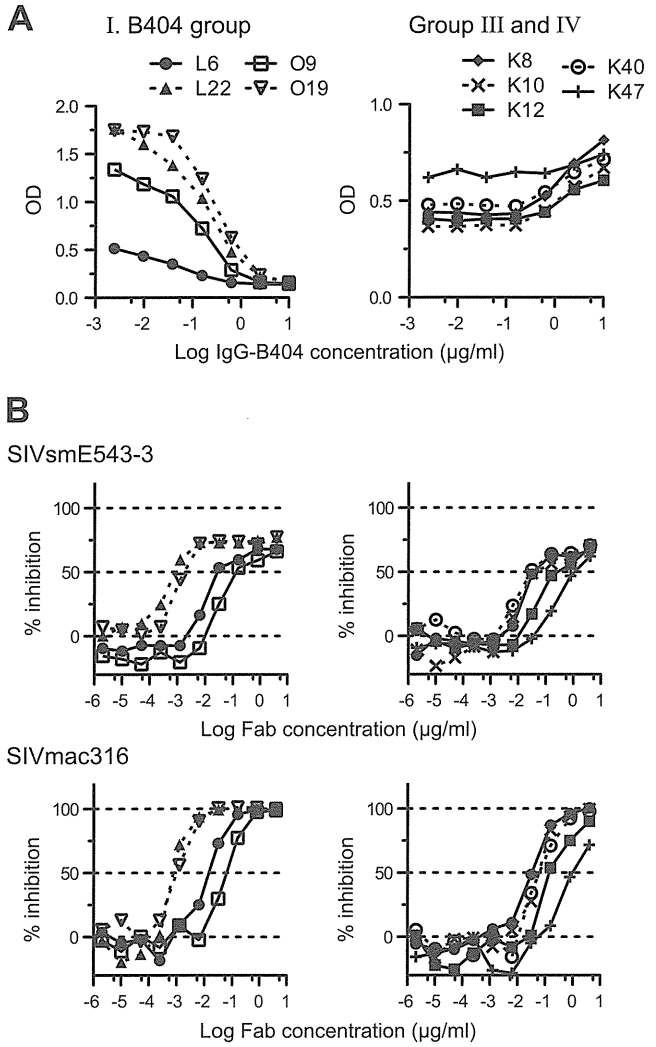


FIG 4 The specificity and potency of Fab clones in the B404 group are similar to those of B404. (A) Competition ELISA was performed using serially diluted B404 IgG as a competitor. B404 IgG significantly inhibited the binding of the Fabs in the B404 group (L6, L22, O9, and O19). In contrast, B404 IgG did not compete with the Fabs in groups III (K8 and K10) and IV (K12, K40, and K47) and even enhanced the binding of these Fabs. (B) Neutralization potencies of Fabs in the B404 group (left) and groups III and IV (right) are shown by inhibition of infection to TZM-bl cells with neutralization-resistant SIVsmE543-3 and genetically divergent SIVmac316.

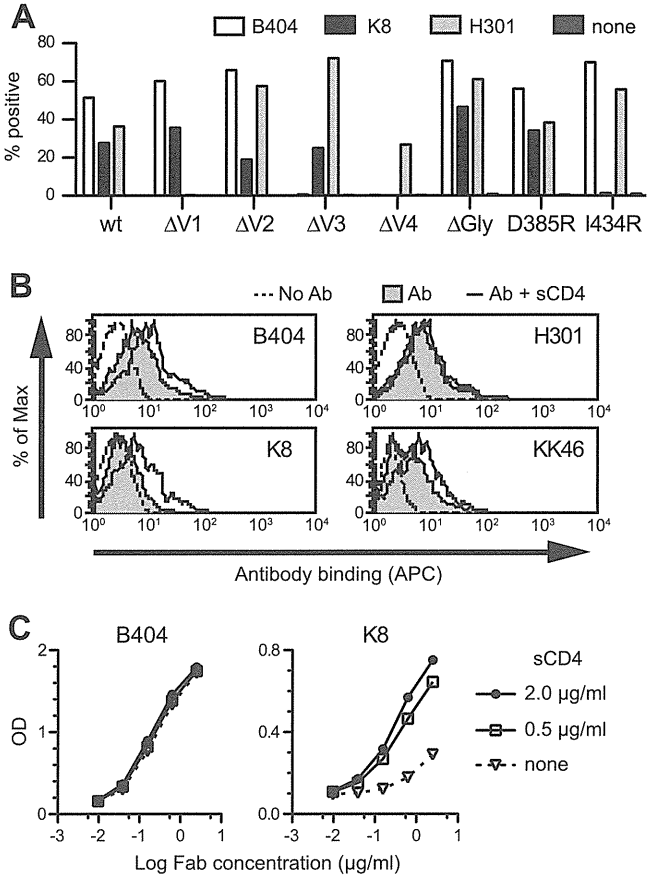


FIG 5 B404 recognizes a conformational epitope, including the V3 and V4 loops, and sCD4 enhances the exposure of the epitope in trimeric Env. (A) Reactivity of B404, K8, and H301 (anti-V1 Fab) to Env mutants was examined using 293T cells transfected with plasmids to express SIVsmE543-3 Env (wild-type), mutants with deletions in the V1 (ΔV1), V2 (ΔV2), V3 (ΔV3), and V4 (ΔV4) loops, an N306A/N316A/N349A mutant lacking glycosylation sites near the V3 loop (ΔGly), a D385R mutant interfering with CD4bs antibodies (D385R), and an I434R mutant interfering with CD4i antibodies (I434R). The transfected cells were stained with Fabs B404, K8, and H301, and the reactivity of Env mutants was analyzed using flow cytometry. The percentage of Fab$^+$ cells is shown. (B) Reactivity of Fabs B404, K8, and H301, and murine anti-V3 MAb KK46 to sCD4-treated trimeric Env on the cell surface. Cells transfected with the plasmid to express SIVsmE543-3 Env were incubated with 2 μg/ml sCD4 for 15 min, and the reactivities of antibodies were similarly examined. The tinted histogram represents cells stained by antibody in the absence of sCD4. The dotted line shows the unstained control. (C) Reactivity of Fab clones B404 and K8 to sCD4-treated monomeric Env. The reactivity of serially diluted Fab to Env was examined by ELISA using SIVsmE543-3 as an antigen in the absence or presence of 0.5 or 2.0 μg/ml sCD4.

tant lacking 3 glycosylation sites flanking the V3 loop (ΔGly) were constructed. In addition, mutants carrying single mutations in the CD4bs (D385R) and CD4i (I434R) sites, corresponding to D368R and I420R in HIV-1 gp120 (13, 44–46), were examined to clarify the relationship of the B404 epitope to the CD4bs and CD4i sites. Flow cytometry analysis using cells expressing these Env mutants revealed that the reactivity of B404 was completely lost in ΔV3 and ΔV4 mutants, though B404 bound to other mutants even better than it did to the wild type (Fig. 5A). These results suggested that B404 recognizes a conformational epitope consisting of the V3 and V4 loops.

The reactivity of another Fab, K8, which targets an epitope other than that of B404 (Fig. 4A), was lost in ΔV4 and I434R mutants (Fig. 5A). No reactivity to I434R strongly suggested that K8 is a CD4i antibody. Therefore, the effect of sCD4 ligation on antibody binding to Env trimers and monomers was examined using flow cytometry and ELISA, respectively. The reactivity of B404, K8, and KK46 (murine anti-V3 MAb) to Env on the cell surface was enhanced by the addition of sCD4, although no effect was observed in anti-V1 Fab H301 (Fig. 5B). This suggested that epitopes for B404, K8, and KK46 are exposed in the open conformation of the Env trimer triggered by CD4 binding. Consistent with the analysis of mutant Envs, the reactivity of K8 to Env monomer was enhanced by the addition of sCD4, but B404 showed no enhancement of reactivity (Fig. 5C).

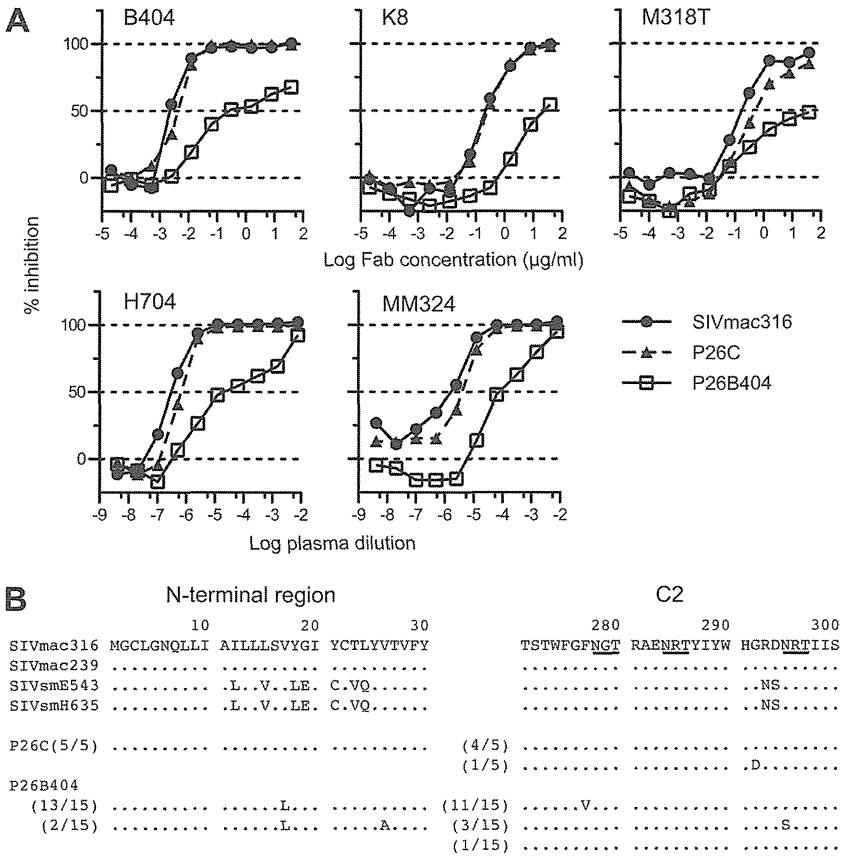


FIG 6 Isolation of variants resistant to B404 and amino acid substitutions in gp120. The B404-resistant variant was induced from SIVmac316 by passages of viruses in PM-1/CCR5 cells with increasing concentrations of B404 Fab. A B404-resistant variant, P26B404, was obtained from the supernatant of passage 26. P26C was obtained after 26 passages without B404. (A) The sensitivities of P26B404, P26C, and parental SIVmac316 to neutralization are shown by inhibition of infection of TZM-bl cells. B404 and K8 Fabs, murine MAb M318T, which recognizes the V2 of gp120, and plasma samples from SIVsmH635FC-infected macaque H704 and SIVmac239-infected macaque MM324 were used for the neutralization assay. (B) Amino acid sequences of the N-terminal and C2 regions of gp120 from P26C and P26B404 are aligned with those of parental SIVmac316 and SIV strains, SIVmac239, SIVsmE543-3 and SIVsmH635FC. The number of clones per total number of clones is given in parentheses. Identical amino acids are shown as dots, and potential glycosylation sites in SIVmac316 are indicated with underlining.

The enhancement by sCD4 of reactivity to both monomeric and trimeric Env and the interference in binding by the I434R (I420R in HIV-1) mutation in Env, which are features of so-called CD4i antibodies against HIV-1 (13, 45, 46), indicate that K8 targets the CD4i epitope. The enhanced reactivity of B404 by sCD4 to trimeric but not monomeric Env is analogous to the reactivity of anti-V3 antibodies (65). These results suggest that B404 recognizes a conformational epitope consisting of the V3 and V4 loops, which are intensely exposed on the Env trimer after CD4 ligation.

**Selection of variants resistant to NAb B404.** To select B404-resistant variants *in vitro*, we passaged SIVmac316, which is the most sensitive to B404 of the SIV strains tested (Fig. 1), in PM1/CCR5 cells in the presence of increasing concentrations of B404. As a control, passage under the same conditions without B404 was also performed to monitor spontaneous changes during infection in PM1/CCR5 cells. The concentration of B404 was increased from 5 ng/ml to 400 μg/ml at passage 26. Viruses recovered at passage 26 in the presence and absence of B404, which were designated P26B404 and P26C, respectively, were examined for their sensitivity to antibodies and plasma samples from SIV-infected macaques (Fig. 6A). The $IC_{50}$ for B404 against SIVmac316, P26C, and P26B404 were 2.8, 4.1, and 240 ng/ml, respectively, showing an 86-fold resistance of P26B404 to B404 compared with that of wild-type SIVmac316. P26B404 was also resistant to neutralization by MAbs K8 (CD4i) and M318T (V2), which target epitopes other than that of B404, and plasma samples from SIV-infected macaques (Fig. 6A). These results suggested that P26B404 acquired resistance to antibody-mediated neutralization comparable to that observed in neutralization-resistant SIV strains, such as SIVmac239 and SIVsmE543-3. Sequence analysis of gp120 revealed 3 amino acid substitutions specific to P26B404: V17L in the N-terminal region and F277V and N295S in the C2 region (Fig. 6B). Of these substitutions, the two in the C2 region were highly conserved among SIVsm/mac and HIV-2 strains. These substitutions were independently observed, and no variant with both F277V and N295S was found in the 15 clones sequenced.

**MD simulation of gp120 outer domains from B404-sensitive and B404-resistant variants.** To address structural impacts of the 2 mutations in the C2 region, we performed MD simulation of unliganded gp120 outer domains from B404-sensitive (SIVmac316) and B404-resistant (F277V and N295S) variants. To map the sites at which structural dynamics were influenced by C2 mutations, we calculated the RMSF of the main chains of individual amino acid residues using 90,000 snapshots from 5 to 50 ns of

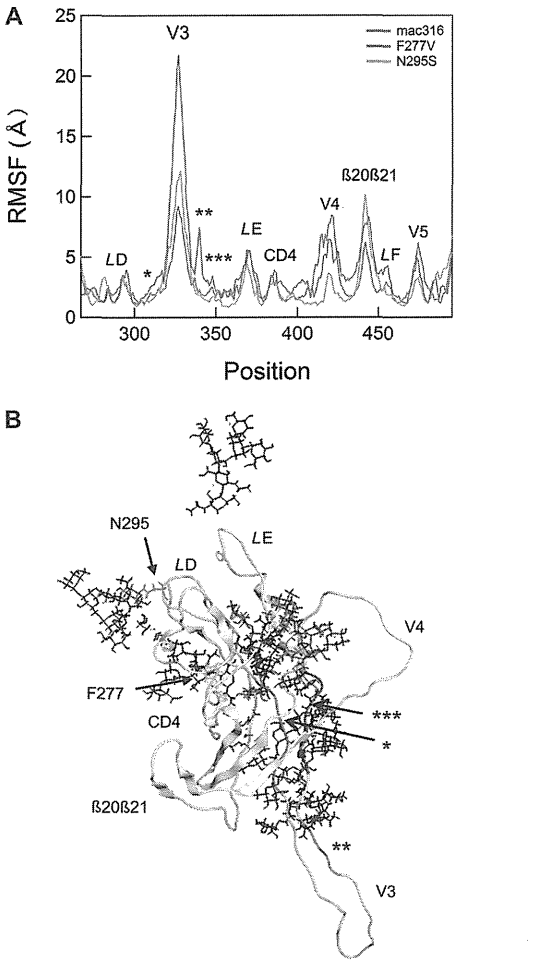


FIG 7 Effects of F277V and N295S mutations on the structural dynamics of the gp120 outer domain. (A) Distribution of RMSF in the gp120 outer domain. MD simulations of gp120 outer domains of SIVmac316, F277V, and N295S were carried out at 1 atm and 310 K for 50 ns as described in Materials and Methods. The RMSF values, which indicate the atomic fluctuations of the main chains of individual amino acids during MD simulations, were calculated using 90,000 snapshots from 9 to 50 ns of each MD simulation. The numbers on the horizontal axes indicate amino acid positions in gp120. The RMSF values of the mutants are significantly different from those of parental SIVmac316 at the V3 loop, the V3 flanking regions (indicated by asterisks), the V4 loop, the β20β21/*LF* loop, and the V5 loop regions. (B) A structure at 50 ns of MD simulation of the SIVmac316 gp120 outer domain is shown as a representative to indicate the steric location of mutation sites and various loops. The regions that are proximal to the V3/V4 loops and displayed fluctuations that differed from those of parental SIVmac316 (Fig. 7A) are highlighted in orange (*), blue (**), and purple (***). Green sticks indicate glycans.

each MD simulation (Fig. 7A). RMSF values provide key information about the atomic fluctuations of the individual amino acids of a protein in solution (57). These values were maximal at the tip of the V3 loop and prominent at other loop regions, including *LD*, *LE*, CD4 binding, V4, β20β21/*LF*, and V5 (Fig. 7A), suggesting that these loops fluctuate in solution. Notably, the F277V and N295S mutations were found to induce changes in RMSF values mainly at the V3, V4, β20β21/*LF*, and V5 loop regions (Fig. 7A, blue and green lines, respectively). Interestingly, these regions are located far from the C2 mutation sites compared with the locations of other loops, such as *LD*, *LE*, and CD4 binding, which had RMSF values that were similar among wild-type and B404-resistant variants (Fig. 7B; F277V in *LD* and N295S in the proximal region of *LD*). In particular, RMSF changes by the C2 mutations were the most prominent at the V3/V4 loops and their neighboring regions (Fig. 7). These results suggested that the F277V and N295S mutations could alter the structural dynamics of V3/V4 loops and their neighboring regions in solution. The structural alterations would lead to changes in entropy of the regions, which affect the binding affinity to B404. The finding is consistent with the results of an epitope mapping study of B404.

## DISCUSSION

Potent and broadly neutralizing MAbs have recently been isolated from HIV-1-infected patients and analyzed to understand the mechanism of neutralization against a broad spectrum of HIV-1 strains and to design vaccines against their neutralizing epitopes (12–16). Although the SIV-macaque model has been used as an animal model for HIV-1 infection for vaccine development (6, 8, 24), no potent and broadly neutralizing monoclonal antibody against SIV was available. Therefore, the epitopes and mechanism for broad neutralization of SIV remained uncertain. Many monoclonal antibodies against SIVsm/mac were isolated from SIV-infected macaques (66, 67) and mice immunized with SIV Env (43, 47, 68), but few of them showed neutralizing activity against various SIV strains, including highly neutralization-resistant SIVmac239 (68). In comparison with these monoclonal antibodies against SIV identified so far, B404 apparently has a broadly neutralizing activity, which enables it to neutralize multiple, diverse SIV isolates, and can be defined as the first generation of broadly NAbs against SIV. The broad and potent neutralizing activity of B404 shown in this study indicates that B404 can be used to analyze broad neutralization against SIV. The B404 epitope, the newly identified broadly neutralizing epitope against SIV, will further understanding of the mechanism of broad neutralization effective for protection from SIV infection.

The infection of rhesus macaques with SIVsmH635FC, a highly neutralization-sensitive clone, was chosen for this study because this SIV strain induced a vigorous and potent antibody response in all the infected macaques and acquired many viral mutations to escape antibody recognition (25, 26). The kinetics of B404 neutralization against various SIV strains were similar to those observed in the plasma sample of the macaque from which B404 was isolated, suggesting that B404-like NAbs are representative of the neutralizing activity in SIVsmH635-infected macaque H723 (25). Consistent with this observation, B404-like NAbs were shown to be a major group in NAbs genetically and functionally. Most of the NAbs in the 4 SIVsmH635FC-infected macaques analyzed had the same features, including the use of a specific VH3 germ line and λ light chains, a long CDRH3 loop, and competition with B404. The bias in the specificity and gene usage may be partially enhanced by the screening process, because B404-like NAbs were predominantly isolated from λ light-chain libraries by panning against H301-conjugated Env. In addition, isolating antibodies against quaternary epitopes constituted by the Env trimer through panning using monomeric Env was difficult. However, the presence of many independent B404-like NAbs strongly suggests that B404-like NAbs compose a significant fraction of NAbs in 4 SIVsmH635FC-infected macaques. Moreover, the vigorous induction of B404-like NAbs in SIVsmH635FC-infected macaques was also supported by the multiple B cell origins apparent

from several subgroups in B404-like NAbs (Fig. 1). These subgroups originated from distinct B cell precursors generated by VDJ recombination, because they were often distinguished by the length and nucleotide sequences of CDRH3.

The observation of few B404-like NAbs from macaques infected with the SIV mix clearly indicates that induction of B404-like NAbs depends on infection with SIVsmH635FC. The exclusive induction of B404-like NAbs only in SIVsmH635FC-infected macaques also raises the possibility that Env from SIVsmH635FC is a highly immunogenic protein that induces antibodies against the B404 epitope. The use of Env from SIVsmH635FC for vaccination may be advantageous for the induction of broadly neutralizing antibodies, because the Env from an HIV-1-infected patient with broadly neutralizing antibodies induced cross-reactive anti-HIV-1 NAbs in an animal model (69). The Env in this vaccination study is capable of mediating CD4-independent infection. Since the Env of SIVsmH635FC has a mutation in the CD4-binding region (D385N), NAb induction may be affected by CD4 independency of Env. The development of vaccines aimed at inducing B404-like NAbs in rhesus macaques will be useful in establishing models for development of antibody-based vaccines targeting specific epitopes for broad neutralization.

Biased usage of a specific VH3 germ line gene and λ light chain are remarkable genetic features of B404-like NAbs. The induction of NAbs with specific germ line genes, such as VH1-69 for CD4i (70) and VH5-51 for V3 (64), is frequently observed in HIV-1-infected patients. A close relationship between VH germ line genes and target epitopes suggests the importance of Ig gene usage in the induction of broadly neutralizing antibodies. Therefore, rational design of vaccines has been undertaken based on reactivity to antibodies with the germ line genes used by known broadly neutralizing antibodies (11, 71, 72). Unfortunately, the VH3 germ line gene of B404 is divergent from all human VH3 germ line genes, suggesting the absence of a human counterpart. This may partially explain why B404-like NAbs have not been identified in HIV-infected humans, although the structure of HIV-1 Env, which is different from that of SIV, significantly affects immunogenicity of the B404 epitope. Rhesus macaque-specific germ line genes were also used by NAbs against the quaternary epitope of HIV-1 Env from simian and human immunodeficiency virus (SHIV)-infected macaques, but their germ line genes were different from the VH3 germ line gene used by B404 (73). Even in the presence of a human VH gene counterpart, the antibody response to a neutralizing epitope may differ between rhesus macaques and humans (74). In addition to the genetic diversity of germ line genes, the rhesus macaque CDRH3 repertoire differs from that of humans, resulting in species-specific antibody repertoires (75). This species specificity in antibody induction is a problem in the evaluation of HIV-1 vaccines in animal models, especially those designed for specific neutralizing epitopes of HIV-1. Conversely, K8, the CD4i NAb from a SIV-infected macaque, used the rhesus VH1 germ line gene, an analog of human VH1-69 frequently used by CD4i NAbs in HIV-1-infected humans (70). Thus, the mechanism of induction of CD4i NAbs with VH1-69 may be common in both humans and rhesus macaques. To analyze vaccine candidates properly in nonhuman primates, similarities and differences in antibody response between rhesus macaques and humans should be considered.

B404 recognizes a conformational epitope consisting of the V3 and V4 loops. The enhanced exposure of the epitope in trimeric Env by sCD4 and efficient neutralization of neutralization-resistant SIV strains by the scFv form of B404 suggests that the B404 epitope is sterically masked by the V1/V2 loops and glycans, analogous to CD4i and V3 epitopes (46, 65, 76). Consistent with this interpretation, B404 reacted more intensely to Env mutants lacking the V1 and V2 loops than to the wild-type Env. MD simulation supported these observations by indicating changes in the structural dynamics of V3/V4 loops and their neighboring regions in gp120 of resistant variants with F277V and N295S mutations in the C2 region. The acquisition of resistance to the broadly neutralizing antibodies b12, PG9, and PG16 due to C2 mutations far from the target epitopes was also observed in HIV-1 CRF01_AE (77, 78). MD simulation is a powerful computational method for analyzing structural dynamics of proteins in solution on the basis of theoretical and empirical principles in physical chemistry (79) and has been applied to research on viruses (80). The structural dynamics of protein surfaces in solution plays a key role in protein interactions, and MD simulation is advantageous in speculation about interactions between proteins containing flexible regions, such as V3 and V4 loops. Analysis of fluctuation changes in mutant proteins is useful to identify the regions which affect protein-protein interaction.

Although the V3 and V4 loops are known to contain linear epitopes for antibody-mediated neutralization in SIV infection, no conformational MAb against SIV with characteristics similar to those of B404 has been reported (43, 47, 66–68). Several MAbs to conformational epitopes that include the V3 region, such as PGT antibodies, represented by PGT128 (15, 19), 3BC176, and 3BC315 (81), were isolated from HIV-1-infected patients. The PGT128 epitope consists of the short segment of the V3 loop and 2 neighboring glycans (19), but the binding of B404 is independent of these glycans near the V3 region. The epitope of 3BC176 and 3BC315 is close to the V3 loop, and their binding is partially enhanced by CD4 binding, similar to that of B404 (81). However, in contrast to B404, 3BC176 and 3BC315 do not bind to monomeric Env and compete with CD4i antibodies, suggesting that their epitope is different from that of B404. Although we have not determined the precise B404 epitope, the characteristics of B404 that are similar to those of CD4i and V3 antibodies suggest that B404 recognizes a conserved region important for binding to the CCR5 coreceptor (46, 65, 76, 82).

Despite recent progress in understanding the broad neutralization of HIV-1, epitopes for potent and broad neutralization have not been analyzed in an SIV model because NAb analysis using SIV cannot be directly applied to HIV-1. The main disadvantage of SIV is the antigenicity difference relative to HIV-1, which makes examination of neutralizing epitopes of HIV-1 impossible. Although the use of SHIV expressing HIV-1 Env enables the evaluation of vaccine candidates designed for target epitopes of HIV-1 in nonhuman primates, an SIV model was more predictive of vaccine efficacy than a SHIV model in clinical trials of a T-cell-based vaccine (83, 84). For comprehensive assessment of immunity induced by vaccine candidates, proof-of-concept trials using the SIV model should be considered before further efficacy trials. The identification of B404 with its potent and broad neutralizing activity against SIV will be a useful adjunct for evaluating the mechanism of neutralization in an SIV-macaque model and will contribute to the development of HIV-1 vaccines.

## ACKNOWLEDGMENTS

We thank Yuko Katsumata for excellent assistance. The phagemid vector pComb3X was kindly provided by the Scripps Research Institute. The following reagents were obtained through the NIH AIDS Research and Reference Reagent Program, Division of AIDS, NIAID, NIH: TZM-bl cells from John C. Kappes, Xiaoyun Wu, and Tranzyme Inc. and KK46 from Karen Kent and Caroline Powell.

This work was supported in part by the Special Coordination Funds for Promoting Science and Technology, the Program of Founding Research Centres for Emerging and Re-emerging Infectious Diseases, the Global COE program Global Education and Research Centre Aiming at the Control of AIDS, a grant-in-aid for scientific research (C-24591484) from the Ministry of Education, Culture, Sport, Science and Technology, Japan, and a grant from the Ministry of Health, Welfare and Labor of Japan (H24-AIDS-007).

## REFERENCES

1. **Igarashi T, Brown C, Azadegan A, Haigwood N, Dimitrov D, Martin MA, Shibata R.** 1999. Human immunodeficiency virus type 1 neutralizing antibodies accelerate clearance of cell-free virions from blood plasma. Nat. Med. 5:211–216.
2. **Shibata R, Igarashi T, Haigwood N, Buckler-White A, Ogert R, Ross W, Willey R, Cho MW, Martin MA.** 1999. Neutralizing antibody directed against the HIV-1 envelope glycoprotein can completely block HIV-1/SIV chimeric virus infections of macaque monkeys. Nat. Med. 5:204–210.
3. **Veazey RS, Shattock RJ, Pope M, Kirijan JC, Jones J, Hu Q, Ketas T, Marx PA, Klasse PJ, Burton DR, Moore JP.** 2003. Prevention of virus transmission to macaque monkeys by a vaginally applied monoclonal antibody to HIV-1 gp120. Nat. Med. 9:343–346.
4. **Hessell AJ, Rakasz EG, Poignard P, Hangartner L, Landucci G, Forthal DN, Koff WC, Watkins DI, Burton DR.** 2009. Broadly neutralizing human anti-HIV antibody 2G12 is effective in protection against mucosal SHIV challenge even at low serum neutralizing titers. PLoS Pathog. 5:e1000433. doi:10.1371/journal.ppat.1000433.
5. **Mascola JR, Stiegler G, VanCott TC, Katinger H, Carpenter CB, Hanson CE, Beary H, Hayes D, Frankel SS, Birx DL, Lewis MG.** 2000. Protection of macaques against vaginal transmission of a pathogenic HIV-1/SIV chimeric virus by passive infusion of neutralizing antibodies. Nat. Med. 6:207–210.
6. **Ourmanov I, Kuwata T, Goeken R, Goldstein S, Iyengar R, Buckler-White A, Lafont B, Hirsch VM.** 2009. Improved survival in rhesus macaques immunized with modified vaccinia virus Ankara recombinants expressing simian immunodeficiency virus envelope correlates with reduction in memory CD4+ T-cell loss and higher titers of neutralizing antibody. J. Virol. 83:5388–5400.
7. **Bogers WM, Davis D, Baak I, Kan E, Hofman S, Sun Y, Mortier D, Lian Y, Oostermeijer H, Fagrouch Z, Dubbes R, van der Maas M, Mooij P, Koopman G, Verschoor E, Langedijk JP, Zhao J, Brocca-Cofano E, Robert-Guroff M, Srivastava I, Barnett S, Heeney JL.** 2008. Systemic neutralizing antibodies induced by long interval mucosally primed systemically boosted immunization correlate with protection from mucosal SHIV challenge. Virology 382:217–225.
8. **Flatz L, Cheng C, Wang L, Foulds KE, Ko SY, Kong WP, Roychoudhuri R, Shi W, Bao S, Todd JP, Asmal M, Shen L, Donaldson M, Schmidt SD, Gall JG, Pinschewer DD, Letvin NL, Rao S, Mascola JR, Roederer M, Nabel GJ.** 2012. Gene-based vaccination with a mismatched envelope protects against simian immunodeficiency virus infection in nonhuman primates. J. Virol. 86:7760–7770.
9. **Thorner AR, Barouch DH.** 2007. HIV-1 vaccine development: progress and prospects. Curr. Infect. Dis. Rep. 9:71–75.
10. **McMichael AJ.** 2006. HIV vaccines. Annu. Rev. Immunol. 24:227–255.
11. **Burton DR, Poignard P, Stanfield RL, Wilson IA.** 2012. Broadly neutralizing antibodies present new prospects to counter highly antigenically diverse viruses. Science 337:183–186.
12. **D'Souza MP, Livnat D, Bradac JA, Bridges SH.** 1997. Evaluation of monoclonal antibodies to human immunodeficiency virus type 1 primary isolates by neutralization assays: performance criteria for selecting candidate antibodies for clinical trials. AIDS Clinical Trials Group Antibody Selection Working Group. J. Infect. Dis. 175:1056–1062.
13. **Scheid JF, Mouquet H, Feldhahn N, Seaman MS, Velinzon K, Pietzsch J, Ott RG, Anthony RM, Zebroski H, Hurley A, Phogat A, Chakrabarti B, Li Y, Connors M, Pereyra F, Walker BD, Wardemann H, Ho D, Wyatt RT, Mascola JR, Ravetch JV, Nussenzweig MC.** 2009. Broad diversity of neutralizing antibodies isolated from memory B cells in HIV-infected individuals. Nature 458:636–640.
14. **Walker LM, Phogat SK, Chan-Hui PY, Wagner D, Phung P, Goss JL, Wrin T, Simek MD, Fling S, Mitcham JL, Lehrman JK, Priddy FH, Olsen OA, Frey SM, Hammond PW, Kaminsky S, Zamb T, Moyle M, Koff WC, Poignard P, Burton DR.** 2009. Broad and potent neutralizing antibodies from an African donor reveal a new HIV-1 vaccine target. Science 326:285–289.
15. **Walker LM, Huber M, Doores KJ, Falkowska E, Pejchal R, Julien JP, Wang SK, Ramos A, Chan-Hui PY, Moyle M, Mitcham JL, Hammond PW, Olsen OA, Phung P, Fling S, Wong CH, Phogat S, Wrin T, Simek MD, Protocol GPI, Koff WC, Wilson IA, Burton DR, Poignard P.** 2011. Broad neutralization coverage of HIV by multiple highly potent antibodies. Nature 477:466–470.
16. **Huang J, Ofek G, Laub L, Louder MK, Doria-Rose NA, Longo NS, Imamichi H, Bailer RT, Chakrabarti B, Sharma SK, Alam SM, Wang T, Yang Y, Zhang B, Migueles SA, Wyatt R, Haynes BF, Kwong PD, Mascola JR, Connors M.** 2012. Broad and potent neutralization of HIV-1 by a gp41-specific human antibody. Nature 491:406–412.
17. **Zhou T, Georgiev I, Wu X, Yang ZY, Dai K, Finzi A, Kwon YD, Scheid JF, Shi W, Xu L, Yang Y, Zhu J, Nussenzweig MC, Sodroski J, Shapiro L, Nabel GJ, Mascola JR, Kwong PD.** 2010. Structural basis for broad and potent neutralization of HIV-1 by antibody VRC01. Science 329:811–817.
18. **McLellan JS, Pancera M, Carrico C, Gorman J, Julien JP, Khayat R, Louder R, Pejchal R, Sastry M, Dai K, O'Dell S, Patel N, Shahzad-ul Hussan S, Yang Y, Zhang B, Zhou T, Zhu J, Boyington JC, Chuang GY, Diwanji D, Georgiev I, Kwon YD, Lee D, Louder MK, Moquin S, Schmidt SD, Yang ZY, Bonsignori M, Crump JA, Kapiga SH, Sam NE, Haynes BF, Burton DR, Koff WC, Walker LM, Phogat S, Wyatt R, Orwenyo J, Wang LX, Arthos J, Bewley CA, Mascola JR, Nabel GJ, Schief WR, Ward AB, Wilson IA, Kwong PD.** 2011. Structure of HIV-1 gp120 V1/V2 domain with broadly neutralizing antibody PG9. Nature 480:336–343.
19. **Pejchal R, Doores KJ, Walker LM, Khayat R, Huang PS, Wang SK, Stanfield RL, Julien JP, Ramos A, Crispin M, Depetris R, Katpally U, Marozsan A, Cupo A, Maloveste S, Liu Y, McBride R, Ito Y, Sanders RW, Ogohara C, Paulson JC, Feizi T, Scanlan CN, Wong CH, Moore JP, Olson WC, Ward AB, Poignard P, Schief WR, Burton DR, Wilson IA.** 2011. A potent and broad neutralizing antibody recognizes and penetrates the HIV glycan shield. Science 334:1097–1103.
20. **Ryu SE, Hendrickson WA.** 2012. Structure and design of broadly-neutralizing antibodies against HIV. Mol. Cells 34:231–237.
21. **Stamatatos L, Morris L, Burton DR, Mascola JR.** 2009. Neutralizing antibodies generated during natural HIV-1 infection: good news for an HIV-1 vaccine? Nat. Med. 15:866–870.
22. **Saunders KO, Rudicell RS, Nabel GJ.** 2012. The design and evaluation of HIV-1 vaccines. AIDS 26:1293–1302.
23. **Haynes BF, Kelsoe G, Harrison SC, Kepler TB.** 2012. B-cell-lineage immunogen design in vaccine development with HIV-1 as a case study. Nat. Biotechnol. 30:423–433.
24. **Barouch DH, Liu J, Li H, Maxfield LF, Abbink P, Lynch DM, Iampietro MJ, SanMiguel A, Seaman MS, Ferrari G, Forthal DN, Ourmanov I, Hirsch VM, Carville A, Mansfield KG, Stablein D, Pau MG, Schuitemaker H, Sadoff JC, Billings EA, Rao M, Robb ML, Kim JH, Marovich MA, Goudsmit J, Michael NL.** 2012. Vaccine protection against acquisition of neutralization-resistant SIV challenges in rhesus monkeys. Nature 482:89–93.
25. **Kuwata T, Katsumata Y, Takaki K, Miura T, Igarashi T.** 2011. Isolation of potent neutralizing monoclonal antibodies from an SIV-Infected rhesus macaque by phage display. AIDS Res. Hum. Retroviruses 27:487–500.
26. **Kuwata T, Byrum R, Whitted S, Goeken R, Buckler-White A, Plishka R, Iyengar R, Hirsch VM.** 2007. A rapid progressor-specific variant clone of simian immunodeficiency virus replicates efficiently in vivo only in the absence of immune responses. J. Virol. 81:8891–8904.
27. **Kuwata T, Dehghani H, Brown CR, Plishka R, Buckler-White A, Igarashi T, Mattapallil J, Roederer M, Hirsch VM.** 2006. Infectious molecular clones from a simian immunodeficiency virus-infected rapid-progressor (RP) macaque: evidence of differential selection of RP-specific envelope mutations in vitro and in vivo. J. Virol. 80:1463–1475.
28. **Lusso P, Cocchi F, Balotta C, Markham PD, Louie A, Farci P, Pal R, Gallo RC, Reitz MS, Jr.** 1995. Growth of macrophage-tropic and primary

human immunodeficiency virus type 1 (HIV-1) isolates in a unique CD4+ T-cell clone (PM1): failure to downregulate CD4 and to interfere with cell-line-tropic HIV-1. J. Virol. 69:3712–3720.
29. Yusa K, Maeda Y, Fujioka A, Monde K, Harada S. 2005. Isolation of TAK-779-resistant HIV-1 from an R5 HIV-1 GP120 V3 loop library. J. Biol. Chem. 280:30083–30090.
30. Takeuchi Y, McClure MO, Pizzato M. 2008. Identification of gammaretroviruses constitutively released from cell lines used for human immunodeficiency virus research. J. Virol. 82:12585–12588.
31. Wei X, Decker JM, Liu H, Zhang Z, Arani RB, Kilby JM, Saag MS, Wu X, Shaw GM, Kappes JC. 2002. Emergence of resistant human immunodeficiency virus type 1 in patients receiving fusion inhibitor (T-20) monotherapy. Antimicrob. Agents Chemother. 46:1896–1905.
32. Derdeyn CA, Decker JM, Sfakianos JN, Wu X, O'Brien WA, Ratner L, Kappes JC, Shaw GM, Hunter E. 2000. Sensitivity of human immunodeficiency virus type 1 to the fusion inhibitor T-20 is modulated by coreceptor specificity defined by the V3 loop of gp120. J. Virol. 74:8358–8367.
33. Platt EJ, Wehrly K, Kuhmann SE, Chesebro B, Kabat D. 1998. Effects of CCR5 and CD4 cell surface concentrations on infections by macrophagetropic isolates of human immunodeficiency virus type 1. J. Virol. 72: 2855–2864.
34. DuBridge RB, Tang P, Hsia HC, Leong PM, Miller JH, Calos MP. 1987. Analysis of mutation in human cells by using an Epstein-Barr virus shuttle system. Mol. Cell. Biol. 7:379–387.
35. Hirsch V, Adger-Johnson D, Campbell B, Goldstein S, Brown C, Elkins WR, Montefiori DC. 1997. A molecularly cloned, pathogenic, neutralization-resistant simian immunodeficiency virus, SIVsmE543-3. J. Virol. 71: 1608–1620.
36. Kestler H, Kodama T, Ringler D, Marthas M, Pedersen N, Lackner A, Regier D, Sehgal P, Daniel M, King N, et al. 1990. Induction of AIDS in rhesus monkeys by molecularly cloned simian immunodeficiency virus. Science 248:1109–1112.
37. Mori K, Ringler DJ, Kodama T, Desrosiers RC. 1992. Complex determinants of macrophage tropism in env of simian immunodeficiency virus. J. Virol. 66:2067–2075.
38. Wu F, Ourmanov I, Kuwata T, Goeken R, Brown CR, Buckler-White A, Iyengar R, Plishka R, Aoki ST, Hirsch VM. 2012. Sequential evolution and escape from neutralization of simian immunodeficiency virus SIVsmE660 clones in rhesus macaques. J. Virol. 86:8835–8847.
39. Kuwata T, Nishimura Y, Whitted S, Ourmanov I, Brown CR, Dang Q, Buckler-White A, Iyengar R, Brenchley JM, Hirsch VM. 2009. Association of progressive CD4(+) T cell decline in SIV infection with the induction of autoreactive antibodies. PLoS Pathog. 5:e1000372. doi:10.1371/journal.ppat.1000372.
40. Barbas CF, Scott JM, Silverman G, Burton DR. 2001. Phage display: a laboratory manual. Cold Spring Harbor Laboratory Press, Cold Spring Harbor, NY.
41. Robinson JE, Holton D, Liu J, McMurdo H, Murciano A, Gohd R. 1990. A novel enzyme-linked immunosorbent assay (ELISA) for the detection of antibodies to HIV-1 envelope glycoproteins based on immobilization of viral glycoproteins in microtiter wells coated with concanavalin A. J. Immunol. Methods 132:63–71.
42. Kuwata T, Kodama M, Sato A, Suzuki H, Miyazaki Y, Miura T, Hayami M. 2007. Contribution of monocytes to viral replication in macaques during acute infection with simian immunodeficiency virus. AIDS Res. Hum. Retroviruses 23:372–380.
43. Matsumi S, Matsushita S, Yoshimura K, Javaherian K, Takatsuki K. 1995. Neutralizing monoclonal antibody against a external envelope glycoprotein (gp110) of SIVmac251. AIDS Res. Hum. Retroviruses 11:501–508.
44. Olshevsky U, Helseth E, Furman C, Li J, Haseltine W, Sodroski J. 1990. Identification of individual human immunodeficiency virus type 1 gp120 amino acids important for CD4 receptor binding. J. Virol. 64:5701–5707.
45. Walker LM, Simek MD, Priddy F, Gach JS, Wagner D, Zwick MB, Phogat SK, Poignard P, Burton DR. 2010. A limited number of antibody specificities mediate broad and potent serum neutralization in selected HIV-1 infected individuals. PLoS Pathog. 6:e1001028. doi:10.1371/journal.ppat.1001028.
46. Thali M, Moore JP, Furman C, Charles M, Ho DD, Robinson J, Sodroski J. 1993. Characterization of conserved human immunodeficiency virus type 1 gp120 neutralization epitopes exposed upon gp120-CD4 binding. J. Virol. 67:3978–3988.
47. Kent KA, Rud E, Corcoran T, Powell C, Thiriart C, Collignon C, Stott EJ. 1992. Identification of two neutralizing and 8 nonneutralizing epitopes on simian immunodeficiency virus envelope using monoclonal antibodies. AIDS Res. Hum. Retroviruses 8:1147–1151.
48. Hatada M, Yoshimura K, Harada S, Kawanami Y, Shibata J, Matsushita S. 2010. Human immunodeficiency virus type 1 evasion of a neutralizing anti-V3 antibody involves acquisition of a potential glycosylation site in V2. J. Gen. Virol. 91:1335–1345.
49. Yoshimura K, Shibata J, Kimura T, Honda A, Maeda Y, Koito A, Murakami T, Mitsuya H, Matsushita S. 2006. Resistance profile of a neutralizing anti-HIV monoclonal antibody, KD-247, that shows favourable synergism with anti-CCR5 inhibitors. AIDS. 20:2065–2073.
50. Lefranc MP, Giudicelli V, Ginestoux C, Jabado-Michaloud J, Folch G, Bellahcene F, Wu Y, Gemrot E, Brochet X, Lane J, Regnier L, Ehrenmann F, Lefranc G, Duroux P. 2009. IMGT, the international ImMunoGeneTics information system. Nucleic Acids Res. 37:D1006–D1012.
51. Gibbs RA, Rogers J, Katze MG, Bumgarner R, Weinstock GM, Mardis ER, Remington KA, Strausberg RL, Venter JC, Wilson RK, Batzer MA, Bustamante CD, Eichler EE, Hahn MW, Hardison RC, Makova KD, Miller W, Milosavljevic A, Palermo RE, Siepel A, Sikela JM, Attaway T, Bell S, Bernard KE, Buhay CJ, Chandrabose MN, Dao M, Davis C, Delehaunty KD, Ding Y, Dinh HH, Dugan-Rocha S, Fulton LA, Gabisi RA, Garner TT, Godfrey J, Hawes AC, Hernandez J, Hines S, Holder M, Hume J, Jhangiani SN, Joshi V, Khan ZM, Kirkness EF, Cree A, Fowler RG, Lee S, Lewis LR, Li Z, Liu YS, et al. 2007. Evolutionary and biomedical insights from the rhesus macaque genome. Science 316:222–234.
52. Tamura K, Peterson D, Peterson N, Stecher G, Nei M, Kumar S. 2011. MEGA5: molecular evolutionary genetics analysis using maximum likelihood, evolutionary distance, and maximum parsimony methods. Mol. Biol. Evol. 28:2731–2739.
53. Yokoyama M, Naganawa S, Yoshimura K, Matsushita S, Sato H. 2012. Structural dynamics of HIV-1 envelope Gp120 outer domain with V3 loop. PLoS One 7:e37530. doi:10.1371/journal.pone.0037530.
54. Huang C-c, Lam SN, Acharya P, Tang M, Xiang S-H, Hussan SS-u, Stanfield RL, Robinson J, Sodroski J, Wilson IA, Wyatt R, Bewley CA, Kwong PD. 2007. Structures of the CCR5 N terminus and of a tyrosine-sulfated antibody with HIV-1 gp120 and CD4. Science 317:1930–1934.
55. Chen X, Lu M, Poon BK, Wang Q, Ma J. 2009. Structural improvement of unliganded simian immunodeficiency virus gp120 core by normal-mode-based X-ray crystallographic refinement. Acta Crystallogr. D Biol. Crystallogr. 65:339–347.
56. Group W. 2005. GLYCAM web. Complex Carbohydrate Research Center, University of Georgia, Athens, GA.
57. Case DA, Cheatham TE, Darden T, Gohlke H, Luo R, Merz KM, Onufriev A, Simmerling C, Wang B, Woods RJ. 2005. The Amber biomolecular simulation programs. J. Comput. Chem. 26:1668–1688.
58. Pearlman DA, Case DA, Caldwell JW, Ross WS, Cheatham Iii TE, DeBolt S, Ferguson D, Seibel G, Kollman P. 1995. AMBER, a package of computer programs for applying molecular mechanics, normal mode analysis, molecular dynamics and free energy calculations to simulate the structural and energetic properties of molecules. Comput. Phys. Commun. 91:1–41.
59. Hornak V, Abel R, Okur A, Strockbine B, Roitberg A, Simmerling C. 2006. Comparison of multiple Amber force fields and development of improved protein backbone parameters. Proteins 65:712–725.
60. Kirschner KN, Yongye AB, Tschampel SM, González-Outeiriño J, Daniels CR, Foley BL, Woods RJ. 2008. GLYCAM06: a generalizable biomolecular force field. Carbohydrates. J. Comput. Chem. 29:622–655.
61. Jorgensen W, Chandrasekhar J, Madura J, Impey R, Klein M. 1983. Comparison of simple potential functions for simulating liquid water. J. Chem. Phys. 79:926–935.
62. Ryckaert J-P, Ciccotti G, Berendsen HJC. 1977. Numerical integration of the cartesian equations of motion of a system with constraints: molecular dynamics of n-alkanes. J. Comput. Physics 23:327–341.
63. Apetrei C, Kaur A, Lerche NW, Metzger M, Pandrea I, Hardcastle J, Falkenstein S, Bohm R, Koehler J, Traina-Dorge V, Williams T, Staprans S, Plauche G, Veazey RS, McClure H, Lackner AA, Gormus B, Robertson DL, Marx PA. 2005. Molecular epidemiology of simian immunodeficiency virus SIVsm in U.S. primate centers unravels the origin of SIVmac and SIVstm. J. Virol. 79:8991–9005.
64. Gorny MK, Wang XH, Williams C, Volsky B, Revesz K, Witover B, Burda S, Urbanski M, Nyambi P, Krachmarov C, Pinter A, Zolla-Pazner S, Nadas A. 2009. Preferential use of the VH5-51 gene segment by

the human immune response to code for antibodies against the V3 domain of HIV-1. Mol. Immunol. 46:917–926.
65. Yoshimura K, Harada S, Shibata J, Hatada M, Yamada Y, Ochiai C, Tamamura H, Matsushita S. 2010. Enhanced exposure of human immunodeficiency virus type 1 primary isolate neutralization epitopes through binding of CD4 mimetic compounds. J. Virol. 84:7558–7568.
66. Cole KS, Alvarez M, Elliott DH, Lam H, Martin E, Chau T, Micken K, Rowles JL, Clements JE, Murphey-Corb M, Montelaro RC, Robinson JE. 2001. Characterization of neutralization epitopes of simian immunodeficiency virus (SIV) recognized by rhesus monoclonal antibodies derived from monkeys infected with an attenuated SIV strain. Virology 290: 59–73.
67. Glamann J, Burton DR, Parren PW, Ditzel HJ, Kent KA, Arnold C, Montefiori D, Hirsch VM. 1998. Simian immunodeficiency virus (SIV) envelope-specific Fabs with high-level homologous neutralizing activity: recovery from a long-term-nonprogressor SIV-infected macaque. J. Virol. 72:585–592.
68. Edinger AL, Ahuja M, Sung T, Baxter KC, Haggarty B, Doms RW, Hoxie JA. 2000. Characterization and epitope mapping of neutralizing monoclonal antibodies produced by immunization with oligomeric simian immunodeficiency virus envelope protein. J. Virol. 74:7922–7935.
69. Zhang PF, Cham F, Dong M, Choudhary A, Bouma P, Zhang Z, Shao Y, Feng YR, Wang L, Mathy N, Voss G, Broder CC, Quinnan GV, Jr. 2007. Extensively cross-reactive anti-HIV-1 neutralizing antibodies induced by gp140 immunization. Proc. Natl. Acad. Sci. U. S. A. 104:10193–10198.
70. Huang C-c, Venturi M, Majeed S, Moore MJ, Phogat S, Zhang M-Y, Dimitrov DS, Hendrickson WA, Robinson J, Sodroski J, Wyatt R, Choe H, Farzan M, Kwong PD. 2004. Structural basis of tyrosine sulfation and VH-gene usage in antibodies that recognize the HIV type 1 coreceptor-binding site on gp120. Proc. Natl. Acad. Sci. U. S. A. 101:2706–2711.
71. Xiao X, Chen W, Feng Y, Zhu Z, Prabakaran P, Wang Y, Zhang MY, Longo NS, Dimitrov DS. 2009. Germline-like predecessors of broadly neutralizing antibodies lack measurable binding to HIV-1 envelope glycoproteins: implications for evasion of immune responses and design of vaccine immunogens. Biochem. Biophys. Res. Commun. 390:404–409.
72. Chen W, Streaker ED, Russ DE, Feng Y, Prabakaran P, Dimitrov DS. 2012. Characterization of germline antibody libraries from human umbilical cord blood and selection of monoclonal antibodies to viral envelope glycoproteins: implications for mechanisms of immune evasion and design of vaccine immunogens. Biochem. Biophys. Res. Commun. 417: 1164–1169.
73. Robinson JE, Franco K, Elliott DH, Maher MJ, Reyna A, Montefiori DC, Zolla-Pazner S, Gorny MK, Kraft Z, Stamatatos L. 2010. Quaternary epitope specificities of anti-HIV-1 neutralizing antibodies generated in rhesus macaques infected by the simian/human immunodeficiency virus SHIVSF162P4. J. Virol. 84:3443–3453.
74. Yuan T, Li J, Zhang Y, Wang Y, Streaker E, Dimitrov DS, Zhang M-Y. 2011. Putative rhesus macaque germline predecessors of human broadly HIV-neutralizing antibodies: differences from the human counterparts and implications for HIV-1 vaccine development. Vaccine 29:6903–6910.
75. Link JM, Larson JE, Schroeder HW. 2005. Despite extensive similarity in germline DH and JH sequence, the adult rhesus macaque CDR-H3 repertoire differs from human. Mol. Immunol. 42:943–955.
76. Labrijn AF, Poignard P, Raja A, Zwick MB, Delgado K, Franti M, Binley J, Vivona V, Grundner C, Huang Venturi C-CM, Petropoulos CJ, Wrin T, Dimitrov DS, Robinson J, Kwong PD, Wyatt RT, Sodroski J, Burton DR. 2003. Access of antibody molecules to the conserved coreceptor binding site on glycoprotein gp120 is sterically restricted on primary human immunodeficiency virus type 1. J. Virol. 77:10557–10565.
77. Thenin S, Roch E, Samleerat T, Moreau T, Chaillon A, Moreau A, Barin F, Braibant M. 2012. Naturally occurring substitutions of conserved residues in human immunodeficiency virus type 1 variants of different clades are involved in PG9 and PG16 resistance to neutralization. J. Virol. 93: 1495–1505.
78. Utachee P, Nakamura S, Isarangkura-Na-Ayuthaya P, Tokunaga K, Sawanpanyalert P, Ikuta K, Auwanit W, Kameoka M. 2010. Two N-linked glycosylation sites in the V2 and C2 regions of human immunodeficiency virus type 1 CRF01_AE envelope glycoprotein gp120 regulate viral neutralization susceptibility to the human monoclonal antibody specific for the CD4 binding domain. J. Virol. 84:4311–4320.
79. Henzler-Wildman K, Kern D. 2007. Dynamic personalities of proteins. Nature 450:964–972.
80. Ode H, Nakashima M, Kitamura S, Sugiura W, Sato H. 2012. Molecular dynamics simulation in virus research. Front. Microbiol. 3:258.
81. Klein F, Gaebler C, Mouquet H, Sather DN, Lehmann C, Scheid JF, Kraft Z, Liu Y, Pietzsch J, Hurley A, Poignard P, Feizi T, Morris L, Walker BD, Fatkenheuer G, Seaman MS, Stamatatos L, Nussenzweig MC. 2012. Broad neutralization by a combination of antibodies recognizing the CD4 binding site and a new conformational epitope on the HIV-1 envelope protein. J. Exp. Med. 209:1469–1479.
82. Poignard P, Saphire EO, Parren PW, Burton DR. 2001. GP120: biologic aspects of structural features. Annu. Rev. Immunol. 19:253–274.
83. Sekaly RP. 2008. The failed HIV Merck vaccine study: a step back or a launching point for future vaccine development? J. Exp. Med. 205:7–12.
84. Watkins DI, Burton DR, Kallas EG, Moore JP, Koff WC. 2008. Nonhuman primate models and the failure of the Merck HIV-1 vaccine in humans. Nat. Med. 14:617–621.

Bioorganic & Medicinal Chemistry 21 (2013) 2518–2526

Contents lists available at SciVerse ScienceDirect

Bioorganic & Medicinal Chemistry

journal homepage: www.elsevier.com/locate/bmc

# CD4 mimics as HIV entry inhibitors: Lead optimization studies of the aromatic substituents

Tetsuo Narumi [a], Hiroshi Arai [a], Kazuhisa Yoshimura [b,c], Shigeyoshi Harada [b,c], Yuki Hirota [a], Nami Ohashi [a], Chie Hashimoto [a], Wataru Nomura [a], Shuzo Matsushita [b], Hirokazu Tamamura [a,*]

[a] Institute of Biomaterials and Bioengineering, Tokyo Medical and Dental University, Chiyoda-ku, Tokyo 101-0062, Japan
[b] Center for AIDS Research, Kumamoto University, Kumamoto 860-0811, Japan
[c] AIDS Research Center, National Institute of Infectious Diseases, Shinjuku-ku, Tokyo 162-8640, Japan

ARTICLE INFO

*Article history:*
Received 22 January 2013
Revised 25 February 2013
Accepted 26 February 2013
Available online 7 March 2013

*Keywords:*
CD4 mimicry
Conformational change in gp120
HIV entry inhibitor
Envelope protein opener

ABSTRACT

Several CD4 mimics have been reported as HIV-1 entry inhibitors that can intervene in the interaction between a viral envelope glycoprotein gp120 and a cell surface protein CD4. Our previous SAR studies led to a finding of a highly potent analogue **3** with bulky hydrophobic groups on a piperidine moiety. In the present study, the aromatic ring of **3** was modified systematically in an attempt to improve its antiviral activity and CD4 mimicry which induces the conformational changes in gp120 that can render the envelope more sensitive to neutralizing antibodies. Biological assays of the synthetic compounds revealed that the introduction of a fluorine group as a *meta*-substituent of the aromatic ring caused an increase of anti-HIV activity and an enhancement of a CD4 mimicry, and led to a novel compound **13a** that showed twice as potent anti-HIV activity compared to **3** and a substantial increase in a CD4 mimicry even at lower concentrations.



## 1. Introduction

The first step of HIV entry into host cells is the interaction of a viral envelope glycoprotein gp120 with the cell surface protein CD4.[1] Such a viral attachment process is an attractive target for the development of the drugs to prevent the HIV-1 infection of its target cells.[2] Several small molecules including BMS-806,[3] IC-9564[4] and NBDs[5] have been identified that inhibit the viral attachment process by binding to gp120. Recently, we and others have been exploring the potentials of NBDs-derived CD4 mimics as a novel class of HIV entry inhibitors (Fig. 1).[6–8]

Small molecular CD4 mimics identified by an HIV syncytium formation assay showed potent cell fusion and virus cell fusion inhibitory activity against several HIV-1 laboratory and primary isolates.[5] Furthermore, the interaction of CD4 mimics with a highly conserved and functionally important pocket on gp120, known as the 'Phe43 cavity', induces conformational changes in gp120,[9] a process which occurs with unfavorable binding entropy, leading to a favorable enthalpy change similar to those caused by binding of the soluble CD4 binding to gp120. These unique properties render CD4 mimics valuable not only for the development of entry inhibitors, but which also, when combined with neutralizing antibodies function as envelope protein openers-putatively, stimulants.[10]

The structure of the complex formed by NBD-556 (**1**) bound to the gp120 core from an HIV-1 clade C strain (C1086) was recently determined by X-ray analysis (PDB: 3TGS).[11] As expected with molecular modeling by us[8a] and others,[6a] NBD-556 binds with Phe43 cavity with its *p*-chlorophenyl ring inserted into the cavity, and in addition multiple contacts were observed, with Trp112, Val255, Phe382, Ile424, Asn425, Trp427, Gly473, and Val430 of gp120 were observed (Fig. 2). However, no obvious interaction with Arg59 of CD4 was observed, although the salt bridge formation between Arg59 of CD4 and Asp368 of gp120 is a critical interaction of the viral attachment.[12] Based on this binding model, several potent compounds were recently identified.[6c,7]

Prior to those studies, we performed structure–activity relationship (SAR) studies based on the modification of the piperidine moiety of CD4 mimics to interact with Val430 and/or Asp368. These resulted in the discovery of a potent compound **3** which has bulky hydrophobic groups on its piperidine ring, and shows significant anti-HIV activity and lower cytotoxicity than other known CD4 mimics.[8c] Our study of the docking of **3** into the Phe43 cavity of gp120 suggests that the cyclohexyl group of **3** can interact hydrophobically with the isopropyl group of Val430.

We hypothesized that the optimization of the aromatic ring of **3** would lead to an increase of antiviral activity and CD4 mimicry, the latter inducing the conformational changes in gp120. Here, we de-

* Corresponding author. Tel.: +81 3 5280 8036; fax: +81 3 5280 8039.
*E-mail address:* tamamura.mr@tmd.ac.jp (H. Tamamura).

0968-0896/$ - see front matter © 2013 Published by Elsevier Ltd.
http://dx.doi.org/10.1016/j.bmc.2013.02.041

scribe the systematic modification of the aromatic ring of **3** for further optimization to evaluate substituent effects on anti-HIV activity, cytotoxicity and CD4 mimicry.

## 2. Results and discussion

The co-crystal structure of **1** with the gp120 core revealed that the aromatic group of **1** binds to gp120 by several aromatic–aromatic and hydrophobic interactions (Fig. 2). In particular, hydrophobic space surrounded by the hydrophobic amino acid residues Trp112, Val255, Phe382, and Ile424 is likely to be affected by substituents at the *meta*- and *para*-positions of the aromatic ring, and consequently we decided to investigate substituents at these positions (Fig. 3).

Initially, we selected a chlorine or a methyl group to serve as the *para*-substituent of the aromatic group because CD4 mimic compounds such as **1** (NBD-556) with a *p*-chloro substituent, and because **3** showed significant anti-HIV activity compared to other substituents. Further, CD4 mimic structures such as **2** with a *p*-methyl substituent also showed potent anti-HIV activity and exhibits lower cytotoxicity than those with the *p*-chlorophenyl derivatives.[8a] Next, we chose several halogens including F, Cl and Br, to be the *meta*-substituent on the aromatic group since previous SAR studies revealed that the introduction of an appropriate group with an electron-withdrawing ability at the *meta*-position leads to an increase of binding affinity and antiviral activity.[6a] Furthermore, to investigate whether electron withdrawal and hydrophobicity of the *meta*-position are appropriate, the CD4 mimics with a *meta*-methyl substituent, which has electron-donating properties and is similar in size to bromine, were also synthesized. Finally, two piperidine scaffolds (the 2,2,6,6-tetramethylpiperidine **A** and the dicyclohexylpiperidine **B**) were combined with these aromatics via the oxalamide linker.

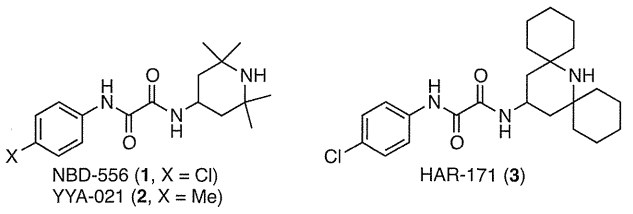


**Figure 1.** Structures of NBD-556 (**1**), YYA-021 (**2**) and HAR-171 (**3**).

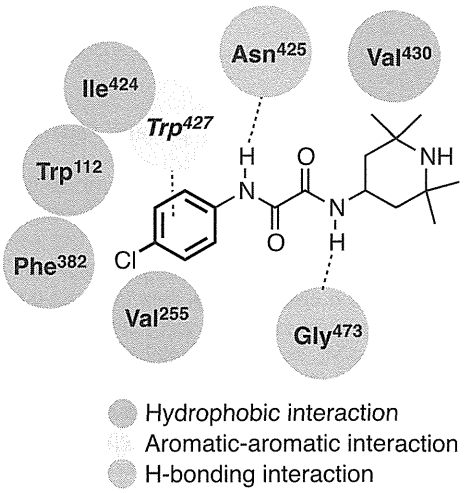


**Figure 2.** Major interactions between NBD-556 and Phe43 cavity of gp120.

### 2.1. Chemistry

The syntheses of novel compounds are depicted in Schemes 1 and 2. Starting from the appropriate aniline with *m*- and *p*-substituents, coupling with ethyl chloroglyoxylate in the presence of $Et_3N$ gave the corresponding amidoesters **6a–c** and **7a–c**. Subsequently, microwave-assisted aminolysis[13] of **6a–c** and **7a–c** with commercially available 4-amino-2,2,6,6-tetramethylpiperidines afforded the desired compounds **8a–c** and **9a–c** (Scheme 1). A series of CD4 mimics with two cyclohexyl groups **13a–c** and **14a–c** were prepared from 2,2,6,6-tetramethylpiperidin-4-one **10** by the method previously reported,[8c] with slight modification (Scheme 2). Briefly, treatment of **10** with cyclohexanone in the presence of ammonium chloride gave a 2,6-substituted piperidin-4-one **11** via Grob fragmentation followed by intramolecular cyclization.[14] Reductive amination with *p*-methoxybenzyl amine, acidic treatment with TMSBr/TFA, and oxidative cleavage of *p*-methoxybenzyl group with cerium(IV) ammonium nitrates (CAN) furnished the corresponding 4-aminopiperidines (**12**) with higher yields and less burdensome purifications than the previous method. Finally, coupling of **12** with the corresponding esters **6a–c** and **7a–c** under microwave irradiation provided the desired compounds **13a–c** and **14a–c**.

### 2.2. Biological evaluation

The anti-HIV activity of the synthetic compounds was evaluated against an R5 primary isolate YTA strain. $IC_{50}$ values were determined by the WST-8 method as the concentrations of the compounds that conferred 50% protection against HIV-1-induced cytopathogenicity in PM1/CCR5 cells. Cytotoxicity of the compounds based on the viability of mock-infected PM1/CCR5 cells was also evaluated using the WST-8 method. The assay results for compounds **8a–c** and **13a–c** with a *p*-chlorophenyl group are shown in Table 1. The parent compound **1** and compound **8a**,[6a] known as JRC-II-191, showed significant anti-HIV activities ($IC_{50}$

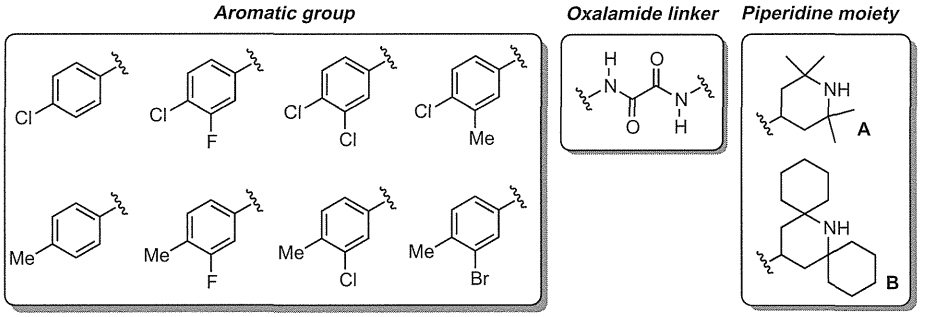


**Figure 3.** The structures of scaffolds in the design of novel CD4 mimics.

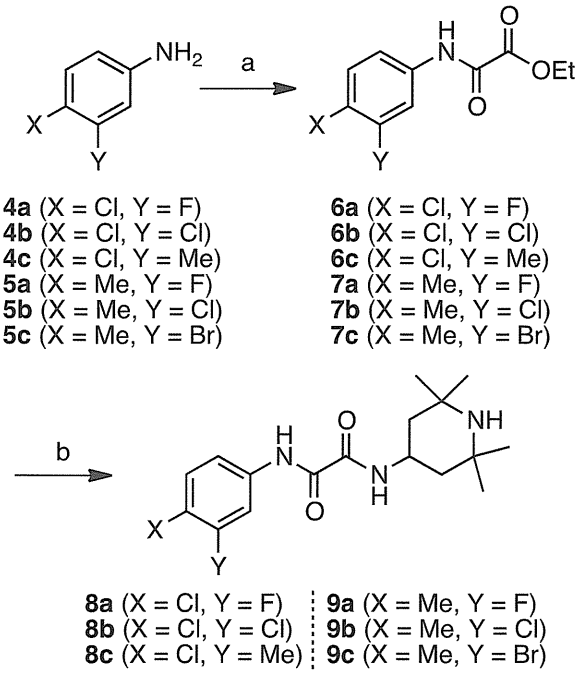


**Scheme 1.** Reagents and conditions: (a) ethyl chloroglyoxylate, $Et_3N$, THF; (b) 4-amino-2,2,6,6-tetramethylpiperidine, $Et_3N$, EtOH, 150 °C, microwave.

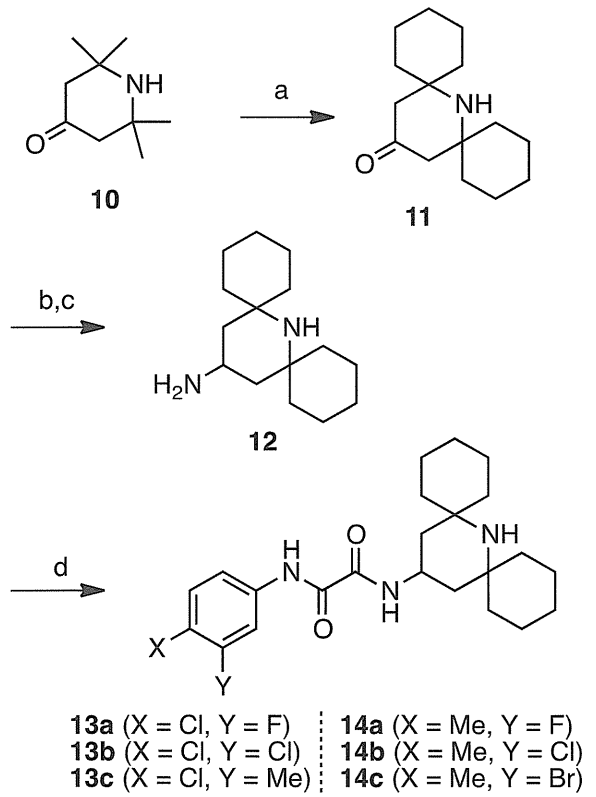


**Scheme 2.** Reagents and conditions: (a) cyclohexanone, $NH_4Cl$, DMSO, 60 °C; (b) *p*-methoxybenzylamine, $NaBH_3CN$, MeOH, then 1 M TMSBr in TFA; (c) CAN, $CH_3CN/H_2O$ (v:v = 2:1); (d) **6** or **7**, $Et_3N$, EtOH, 150 °C, microwave.

of **1** = 0.61 μM and $IC_{50}$ of **8a** = 0.32 μM). Compound **8b**[6a] having a *m*,*p*-dichlorophenyl group and compound **8c**[6a] (JRC-II-193) having a *p*-chloro-*m*-tolyl group showed moderate anti-HIV activity ($IC_{50}$ of **8b** = 4.1 μM and $IC_{50}$ of **8c** = 3.3 μM) but their potency was

**Table 1**
Anti-HIV activity and cytotoxicity of compounds **8a–c** and **13a–c** containing a *p*-chlorophenyl group[a]

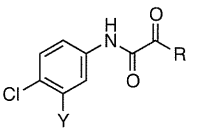


| Compd | R | Y | $IC_{50}$[b] (μM) YTA48P | $CC_{50}$[c] (μM) |
|---|---|---|---|---|
| **1** | 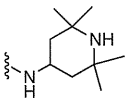 | H | 0.61 | 110 |
| **8a** | **A** | F | 0.32 | 94 |
| **8b** | **A** | Cl | 4.1 | 36 |
| **8c** | **A** | Me | 3.3 | 38 |
| **3** | 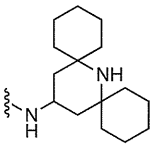 | H | 0.43 | 120 |
| **13a** | **B** | F | 0.23 | 11 |
| **13b** | **B** | Cl | 0.62 | 11 |
| **13c** | **B** | Me | 2.6 | 15 |

[a] All data are the mean values from three of more independent experiments.
[b] $IC_{50}$ values of the multi-round assay are based on the inhibition of HIV-1-induced cytopathogenicity in PM1/CCR5 cells.
[c] $CC_{50}$ values are based on the reduction of the viability of mock-infected PM1/CCR5 cells.

**Table 2**
Anti-HIV activity and cytotoxicity of compounds **9a–c** and **14a–c** containing a *p*-tolyl group[a]

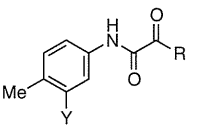


| Compd | R | Y | $IC_{50}$[b] (μM) YTA48P | $CC_{50}$[c] (μM) |
|---|---|---|---|---|
| **2** | 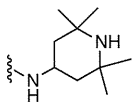 | H | 9.0 | 260 |
| **9a** | **A** | F | 2.8 | 110 |
| **9b** | **A** | Cl | 3.2 | 62 |
| **9c** | **A** | Br | >10 | 32 |
| **14a** | 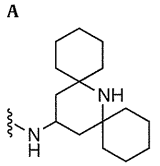 | F | 0.54 | 91 |
| **14b** | **B** | Cl | 6.2 | 11 |
| **14c** | **B** | Br | 3.2 | 11 |

[a] All data are the mean values from three of more independent experiments.
[b] $IC_{50}$ values of the multi-round assay are based on the inhibition of HIV-1-induced cytopathogenicity in PM1/CCR5 cells.
[c] $CC_{50}$ values are based on the reduction of the viability of mock-infected PM1/CCR5 cells.

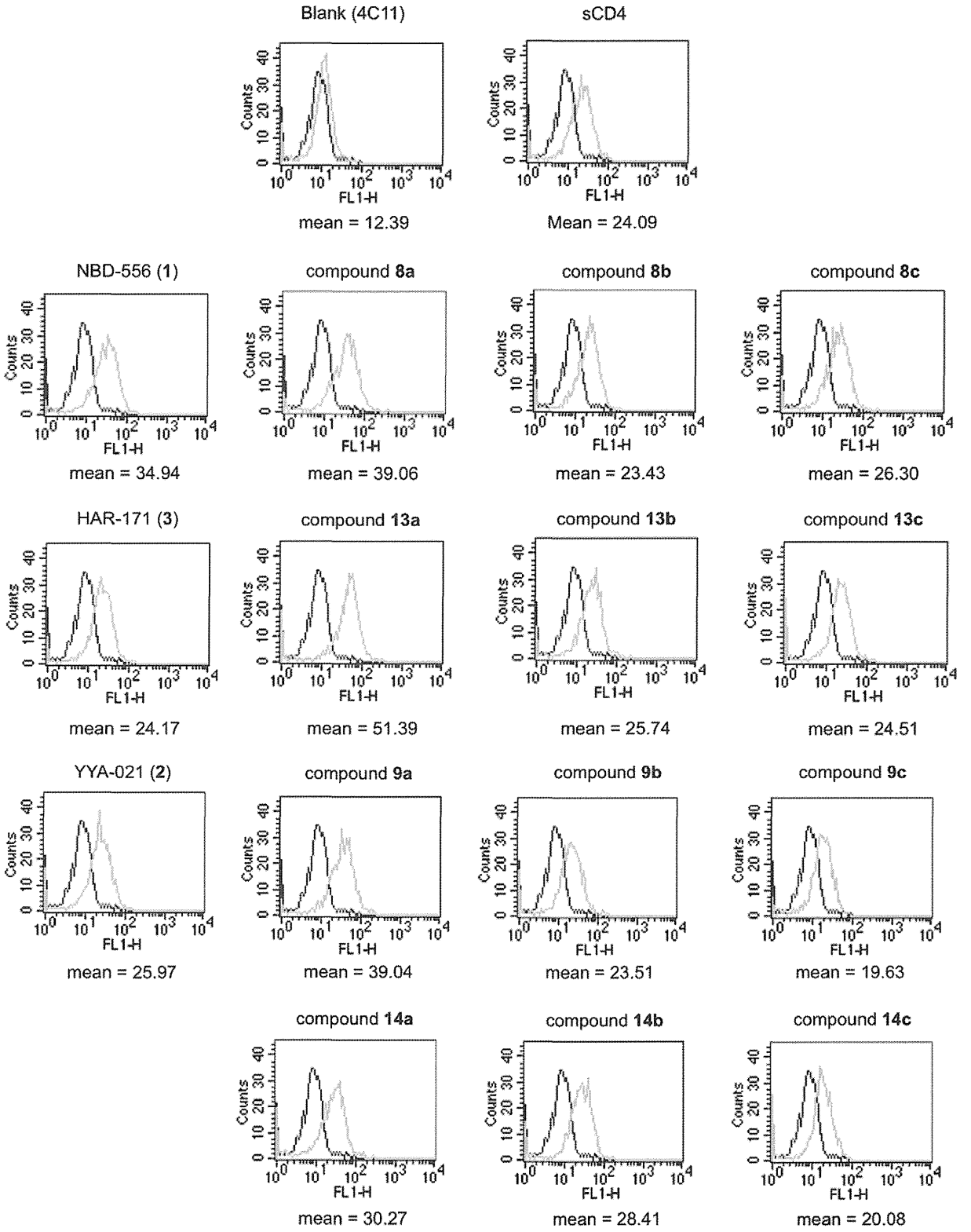


**Figure 4.** FACS analysis of synthetic compounds **8**, **9**, **13** and **14**.

approximately 10-fold lower than that of compound **8a**. The cytotoxicity of **8b** and **8c** is relatively stronger than that of **8a** ($CC_{50}$ of **8b** = 36 μM and $CC_{50}$ of **8c** = 38 μM). Compounds **13a–c** with hydrophobic cyclohexyl groups in the piperidine moiety showed more potent anti-HIV activity than the corresponding compounds **8a–c**, confirming the contribution of the bulky hydrophobic group(s) to an increase of antiviral activity. Our lead compound **3** showed significant anti-HIV activity comparable to that of compound **8a** ($IC_{50}$ = 0.43 μM) but, consistent with previous results, exhibited lower cytotoxicity. In particular, compound **13a** with a *m*-fluoro-*p*-chlorophenyl group exhibited the highest anti-HIV activity. The $IC_{50}$ value of **13a** was 0.23 μM, whose potency was

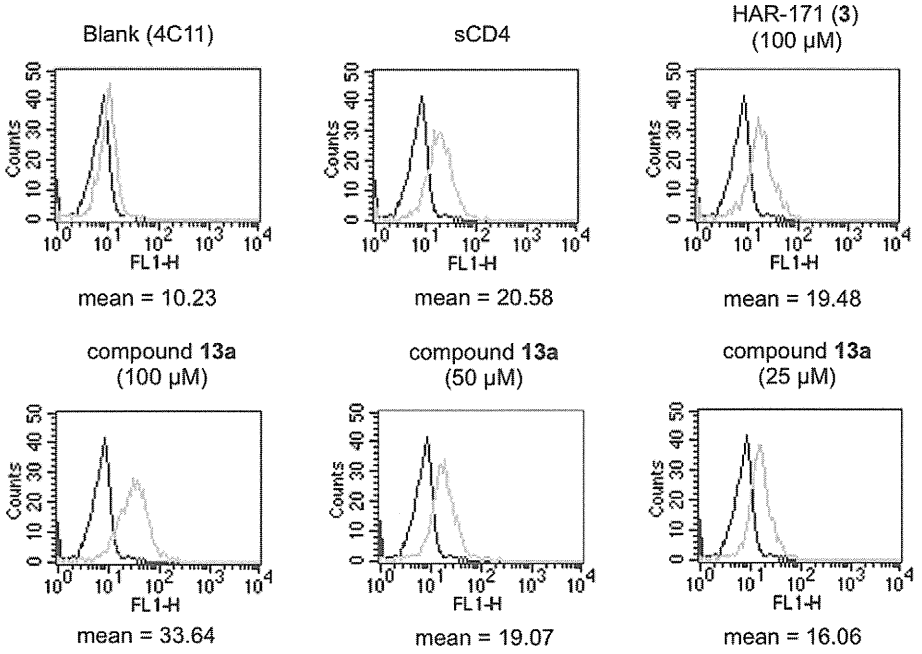


**Figure 5.** FACS analysis of **3** and **13a** in different concentrations.

approximately twice as high as that of compound **3**. Notably, compound **13b** with a *m*,*p*-dichlorophenyl group showed 7-fold more potent anti-HIV activity than the corresponding compound **8b**. Compound **13c**, which has a *p*-chloro-*m*-tolyl group, showed potent anti-HIV activity comparable to that of the corresponding compound **8c** and an increase of cytotoxicity ($CC_{50}$ = 15 μM). We observed a tendency for compounds **13a**–**c** with both hydrophobic cyclohexyl groups and a *m*,*p*-disubstituted phenyl group to exhibit higher cytotoxicity than the corresponding tetramethyl-type compounds **8a**–**c**. No clear reason for an increase of cytotoxicity in the *m*,*p*-disubstituted phenyl group-containing compounds is apparent.

Assay results for the compounds **9a–c** and **14a–c** with a *p*-tolyl group are shown in Table 2. As expected, replacement of the *p*-chloro substituent with a *p*-methyl group resulted in somewhat reduction of anti-HIV activity. Compound **2**, YYA-021 has significant anti-HIV activity ($IC_{50}$ = 9.0 μM) and exhibits the lowest cytotoxicity among all of the compounds tested ($CC_{50}$ = 260 μM). These results are consistent with our previous SAR studies involving the aromatic ring. Introduction of a fluorine at the *meta*-position of the *p*-tolyl group, e.g. in compound **9a** and **14a**, improved the antiviral activity, as observed with **8a** and **13a** and a similar tendency was observed for compound **9b** with a *m*-chloro-*p*-tolyl group. In particular, compound **14a** with cyclohexyl groups and a *m*-fluoro-*p*-tolyl group showed slightly higher anti-HIV activity than the parent compound **1**. Among the compounds with *m*-bromo-*p*-tolyl groups, it was found that compound **9c**, with a 2,2,6,6-tetramethylpiperidine group, showed no anti-HIV activity at a concentration below 10 μM, whereas compound **14c** with hydrophobic cyclohexyl groups attached to the piperidine moiety, showed moderate activity ($IC_{50}$ = 3.2 μM), indicating that the hydrophobic modification of piperidine ring can contribute to an increase in anti-HIV activity.

All the synthetic compounds were evaluated for their CD4 mimicry on the conformational changes in gp120 by fluorescence activated cell sorting (FACS) analysis, and the results are shown in Figure 4. The profile of binding of a CD4-induced (CD4i) monoclonal antibody (4C11) to the Env-expressing cell surface pretreated with the synthetic compounds was assessed in terms of the mean fluorescence intensity (MFI). The increase in binding affinity for 4C11 (by the pretreatment with synthetic compounds) suggests that those compounds can reflect the CD4 mimicry as a consequence of the conformational changes in gp120. Our previous studies disclosed that the profiles of the binding to the cell surface pretreated with **1**, **2**, or **3** were similar to those observed in pretreatment with soluble CD4, indicating that these compounds offer a significant enhancement of binding affinity for 4C11.[8] As shown in Figure 4, similar results were obtained with those compounds in this FACS analysis (MFI of **1**, **2**, and **3** = 34.94, 25.97, and 24.17, respectively). A notable increase in binding affinity for 4C11 was observed in essentially all the synthetic compounds. The compounds **8a**, **9a**, **13a** and **14a** with a *meta*-fluorine in the aromatic ring, showed significant anti-HIV activity, and produced a substantial increase in binding affinity for 4C11. These results suggested that the introduction of a fluorine group at the meta position of the aromatic ring is significant not only for the increase of anti-HIV activity, but also for the enhancement of a CD4 mimicry. In particular, a remarkable improvement in binding affinity for 4C11 was observed with **13a** (MFI = 51.39) which has twofold more potent anti-HIV activity than the lead compound **3** (HAR-171), and is the most active compound in terms of both anti-HIV activity and the CD4 mimicry resulting from the conformational change in gp120. The profiles of pretreatment of the cell surface with compounds **8b** and **13b** having a *m*,*p*-dichlorophenyl group, compounds **8c** and **13c** having a *p*-chloro-*m*-tolyl group, and compounds **9b** and **14b** with a *m*-chloro-*p*-tolyl group were similar to results obtained for **3**, suggesting that these compounds produced slightly lower enhancement compared to those of compounds **8a**, **9a**, **13a** and **14a** but significant levels of binding affinity for 4C11. On the other hand, pretreatment with compounds **9c**, which failed to show significant anti-HIV activity and **14c**, which had moderate anti-HIV activity resulted in a slight decrease of binding affinity for 4C11, suggesting that the introduction of a Br group at the *meta*-position of *p*-tolyl group is not advantageous to a CD4 mimicry, possibly due to the steric hindrance caused by the two bulky substituents. These results are consistent with previous observations that a limited size and electron-withdrawing ability of the aromatic substituents are required for potent anti-HIV activity and CD4 mimicry.[8a]

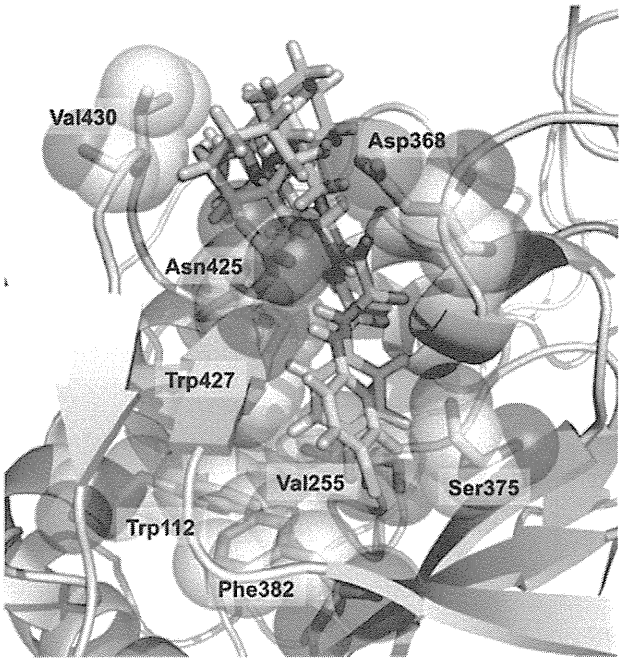


**Figure 6.** The modeled structure of **13a** (yellow carbon atoms) in the complex with the Phe43 cavity in gp120 (3TGS) overlaid with the modeled structure of **3** (green carbon atoms).

Since **13a** showed higher CD4 mimicry than the other compounds tested, the effect of the solution concentration of **13a** on the binding affinity for 4C11 was investigated. As shown in Figure 5, pretreatment of the cell surface with a 100 μM solution of **13a** produced a higher increase in the binding affinity for 4C11 than pretreatment with the same concentration of compound **3**. Interestingly, the profile pretreated with a 50 μM solution of **13a** was similar to that with a 100 μM of compound **3**, and even with a 25 μM solution of **13a** a potent enhancement of the binding affinity for 4C11 was observed: MFI of **13a** at concentrations of 50 μM and 25 μM = 19.07 and 16.06, respectively. This observation suggests that **13a** could serve as a novel lead compound for the development of envelope protein openers for the use combined with neutralizing antibodies because of its effectiveness at low concentrations.

The substantial increase in the CD4 mimicry of **13a** even at a low concentration is not easily explained because HAR-171 (**3**) and **13a** would be expected to form the similar binding modes with gp120. A probable contribution of **13a** is suggested by modeling studies docked into the Phe43 cavity in gp120 (3TGS) in which the depth and direction of the aromatic ring of **13a** is slightly different from those in compound **3** (Fig. 6), leading to the possible formation of appropriate interactions with the hydrophobic amino acid residues such as Val255 and Phe382, and therefore explaining the increased potency observed in the anti-HIV activity and CD4 mimicry of **13a**.

## 3. Conclusion

CD4 mimics are attractive agents not only for the development of a novel class of HIV entry inhibitors but also as possible cooperating agents for the neutralizing antibodies—that is, envelope protein openers. In the present study, a structure–activity relationship study of a series of CD4 mimic compounds was performed with a view to improving the biological activity of HAR-171 (**3**), which was identified in our previous studies as a promising lead compound with anti-HIV activity, cytotoxicity and CD4 mimicry resulting from the conformational change in gp120. Systematic modification of the *meta*- and *para*-substituents of the aromatic ring of **3** led to some potent compounds. In particular, **13a**, which has a bulky hydrophobic group on its piperidine ring and a *m*-fluoro-*p*-chlorophenyl group, demonstrated twofold more potent anti-HIV activity and much higher CD4 mimicry than **2** following the conformational changes in gp120, although the cytotoxicity of **13a** is relatively high. Further structural modification studies of the aromatic ring and the oxalamide linker to improve pharmaceutical profiles will be the subject of future reports.

## 4. Experimentals

$^1$H NMR and $^{13}$C NMR spectra were recorded using a Bruker Avance III spectrometer. Chemical shifts are reported in $\delta$ (ppm) relative to $Me_4Si$ (in $CDCl_3$) as internal standard. Low- and high-resolution mass spectra were recorded on a Bruker Daltonics microTOF focus in the positive and negative detection mode. For flash chromatography, silica gel 60 N (Kanto Chemical Co., Inc.) was employed. Microwave reactions were performed in Biotage Microwave Reaction Kit (sealed vials) in an Initiator™ (Biotage). The wattage was automatically adjusted to maintain the desired temperature for the desired period of time.

### 4.1. Chemistry

#### 4.1.1. Ethyl 2-((4-chloro-3-fluorophenyl)amino)-2-oxoacetate (6a)

To a stirred solution of 3-fluoroaniline (1.11 g, 10.0 mmol) in $CHCl_3$ (30.0 mL) was added dropwise *N*-chlorosuccinimide (NCS) in $CHCl_3$ (20.0 mL) at 0 °C. The mixture was stirred at 0 °C for 42 h. After the reaction mixture was concentrated under reduced pressure, the residue was dissolved in $Et_2O$. The mixture was washed with water, and dried over $MgSO_4$. Concentration under reduced pressure followed by flash chromatography over silica gel with EtOAc/*n*-hexane gave 4-chloro-3-fluoroaniline (259.4 g, 18% yield) as crystalline solids. To a stirred solution of the above aniline (259.4 mg, 1.78 mmol) in THF (8.9 mL) were added at 0 °C ethyl chloroglyoxylate (237.3 μL, 2.14 mmol) and $Et_3N$ (296.6 μL, 2.14 mmol). The mixture was stirred at room temperature for 12 h. After the precipitate was filtrated off, the filtrate solution was concentrated under reduced pressure. The residue was dissolved in EtOAc, and washed with 1.0 M HCl, saturated $NaHCO_3$ and brine, then dried over $MgSO_4$. Concentration under reduced pressure to provide the title compound **6a** (435.2 mg, 99% yield) as brown crystals, which was used without further purification.

$^1$H NMR (500 MHz, $CDCl_3$) $\delta$ 1.44 (t, $J$ = 7.50 Hz, 3H), 4.43 (q, $J$ = 7.50 Hz, 2H), 7.24–7.25 (m, 1H), 7.35–7.40 (m, 1H), 7.70–7.75 (m, 1H), 8.93 (br, 1H); $^{13}$C NMR (125 MHz, $CDCl_3$) $\delta$ 13.0, 64.1, 108.5 (d, $J$ = 26.3 Hz), 115.9 (d, $J$ = 3.75 Hz), 117.3 (d, $J$ = 18.8 Hz), 130.9 (d, $J$ = 10.0 Hz), 135.9, 153.9, 158.1 (d, $J$ = 246.3 Hz), 160.5; HRMS (ESI), *m*/*z* calcd for $C_{10}H_{10}ClFNO_3$ ($MH^-$) 244.0182, found 244.0183.

#### 4.1.2. Ethyl 2-((3,4-dichlorophenyl)amino)-2-oxoacetate (6b)

To a stirred solution of 3,4-dichloroaniline **4b** (1.94 g, 12.0 mmol) in THF (20.0 mL) were added ethyl chloroglyoxylate (1.11 mL, 10.0 mmol) and $Et_3N$ (15.2 mL, 11.0 mmol) at 0 °C. The mixture was stirred at room temperature for 6 h. After the precipitate was filtrated off, the filtrate solution was concentrated under reduced pressure. The residue was dissolved in EtOAc, and washed with 1.0 M HCl, saturated $NaHCO_3$ and brine, then dried over $MgSO_4$. Concentration under reduced pressure to provide the title compound **6b** (1.58 g, 95% yield) as white powder, which was used without further purification.

$^1$H NMR (500 MHz, $CDCl_3$) $\delta$ 1.44 (t, $J$ = 7.00 Hz, 3H), 4.43 (q, $J$ = 7.00 Hz, 2H), 7.44 (d, $J$ = 8.50 Hz, 1H), 7.49–7.51 (m, 1H), 7.87, 2.35 (d, $J$ = 2.50 Hz, 1H); $^{13}$C NMR (125 MHz, $CDCl_3$) $\delta$ 14.0, 64.0, 119.0, 121.5, 129.0, 130.8, 133.2, 135.7, 153.9, 160.5; HRMS (ESI), $m/z$ calcd for $C_{10}H_{10}Cl_2NO_3$ ($MH^+$) 262.0038, found 262.0031.

#### 4.1.3. Ethyl 2-((4-chloro-3-methylphenyl)amino)-2-oxoacetate (6c)

By use of a procedure similar to that described for the preparation of compound **6b**, the aniline **4c** (3.34 g, 24.0 mmol) was converted into the title compound **6c** (4.63 g, 96% yield) as white powder.

$^1$H NMR (500 MHz, $CDCl_3$) $\delta$ 1.43 (t, $J$ = 7.00 Hz, 3H), 2.38 (s, 3H), 4.42 (q, $J$ = 7.00 Hz, 2H), 7.33 (d, $J$ = 8.50 Hz, 1H), 7.43–7.46 (m, 1H), 7.51–7.54 (m, 1H), 8.82 (s, 1H); $^{13}$C NMR (125 MHz, $CDCl_3$) $\delta$ 14.0, 20.2, 63.8, 118.5, 122.0, 129.7, 130.9, 134.8, 137.1, 153.8, 160.9; HRMS (ESI), $m/z$ calcd for $C_{11}H_{13}ClNO_3$ ($MH^+$) 242.0578, found 242.0568.

#### 4.1.4. Ethyl 2-((3-fluoro-4-methylphenyl)amino)-2-oxoacetate (7a)

By use of a procedure similar to that described for the preparation of compound **6b**, the aniline **5a** (3.00 g, 24.0 mmol) was converted into the title compound **7a** (4.24 g, 94% yield) as white powder.

$^1$H NMR (500 MHz, $CDCl_3$) $\delta$ 1.43 (t, $J$ = 7.20 Hz, 3H), 2.25 (s, 3H), 4.42 (q, $J$ = 6.80 Hz, 2H), 7.12–7.21 (m, 2H), 7.48–7.56 (m, 1H), 8.83 (s, 1H); $^{13}$C NMR (125 MHz, $CDCl_3$) $\delta$ 14.2 (2C), 63.8, 107.1 (d, $J$ = 27.5 Hz), 115.0 (d, $J$ = 10.0 Hz), 122.3 (d, $J$ = 17.5 Hz), 131.6 (d, $J$ = 6.25 Hz), 135.3 (d, $J$ = 13.8 Hz), 153.8, 160.8, 161.1 (d, $J$ = 243.8 Hz); HRMS (ESI), $m/z$ calcd for $C_{11}H_{13}FNO_3$ ($MH^+$) 226.0879, found 226.0878.

#### 4.1.5. Ethyl 2-((3-chloro-4-methylphenyl)amino)-2-oxoacetate (7b)

By use of a procedure similar to that described for the preparation of compound **6b**, the aniline **5b** (3.40 g, 24.0 mmol) was converted into the title compound **7b** (5.19 g, 94% yield) as white powder.

$^1$H NMR (500 MHz, $CDCl_3$) $\delta$ 1.43 (t, $J$ = 7.00 Hz, 3H), 2.35 (s, 3H), 4.42 (q, $J$ = 7.00 Hz, 2H), 7.22 (d, $J$ = 8.50 Hz, 1H), 7.41–7.43 (m, 1H), 7.71 (d, $J$ = 2.00 Hz, 1H), 8.83 (s, 1H); $^{13}$C NMR (125 MHz, $CDCl_3$) $\delta$ 14.0, 20.0, 63.8, 118.0, 120.3, 131.2, 133.3, 134.7, 135.0, 153.8, 160.8; HRMS (ESI), $m/z$ calcd for $C_{11}H_{13}ClNO_3$ ($MH^+$) 242.0584, found 242.0573.

#### 4.1.6. Ethyl 2-((3-bromo-4-methylphenyl)amino)-2-oxoacetate (7c)

By use of a procedure similar to that described for the preparation of compound **6b**, the aniline **5c** (4.47 g, 27.0 mmol) was converted into the title compound **7c** (6.24 g, 96% yield) as white powder.

$^1$H NMR (500 MHz, $CDCl_3$) $\delta$ 1.43 (t, $J$ = 7.00 Hz, 3H), 2.38 (s, 3H), 4.42 (q, $J$ = 7.00 Hz, 2H), 7.23 (t, $J$ = 8.50 Hz, 1H), 7.48–7.53 (m, 1H), 7.83–7.90 (m, 1H), 8.80 (s, 1H); $^{13}$C NMR (125 MHz, $CDCl_3$) $\delta$ 14.0, 22.4, 63.9, 118.7, 123.4, 125.0, 131.0, 135.0, 135.2, 153.7, 160.8; HRMS (ESI), $m/z$ calcd for $C_{11}H_{13}BrNO_3$ ($MH^+$) 286.0079, found 286.0068.

#### 4.1.7. $N^1$-(4-Chloro-3-fluorophenyl)-$N^2$-(2,2,6,6-tetramethylpiperidin-4-yl)oxalamide (8a)

To a solution of compound **6a** (70.0 mg, 0.286) in EtOH (2.9 mL) were added $Et_3N$ (0.200 mL, 1.45 mmol) and 2,2,6,6-tetramethylpiperidin-4-amine (0.150 mL, 0.870 mmol). The reaction mixture was stirred for 3 h at 150 °C under microwave irradiation. After being concentrated in vacuo, the residue was extracted with $CHCl_3$, and washed with saturated $NaHCO_3$ and brine, then dried over $MgSO_4$. Concentration under reduced pressure to provide the title compound **8a** (34.6 mg, 34% yield) as white powder.

$^1$H NMR (500 MHz, $CDCl_3$) $\delta$ 0.99–1.50 (m, 15H), 1.92 (dd, $J$ = 3.50, 9.00 Hz, 2H), 4.20–4.32 (m, 1H), 7.21–7.25 (m, 1H), 7.34–7.41 (m, 1H), 7.69–7.73 (m 1H), 9.31 (br, 1H); $^{13}$C NMR (125 MHz, $CDCl_3$) $\delta$ 28.4, 34.8, 43.8, 44.5, 51.0, 108.3 (d, $J$ = 26.3 Hz), 115.8 (d, $J$ = 3.75 Hz), 117.1 (d, $J$ = 17.5 Hz), 130.8, 136.2 (d, $J$ = 8.75 Hz), 157.6, 158.1 (d, $J$ = 247.5 Hz), 158.4; HRMS (ESI), $m/z$ calcd for $C_{17}H_{24}ClFN_3O_2$ ($MH^+$) 356.1536, found 356.1548.

#### 4.1.8. $N^1$-(3,4-Dichlorophenyl)-$N^2$-(2,2,6,6-tetramethylpiperidin-4-yl)oxalamide (8b)

By use of a procedure similar to that described for the preparation of compound **8a**, the compound **6b** (261.0 mg, 1.00 mmol) was converted into the title compound **8b** (520.0 mg, 70% yield) as white powder.

$^1$H NMR (500 MHz, $CDCl_3$) $\delta$ 1.07 (t, $J$ = 12.0 Hz, 2H), 1.16 (s, 6H), 1.28 (s, 6H), 1.90–1.93 (m, 2H), 4.20–4.32 (m, 1H), 7.26 (m, 1H), 7.40–7.48 (m, 2H), 7.88 (s, 1H), 9.33 (s, 1H); $^{13}$C NMR (125 MHz, $CDCl_3$) $\delta$ 28.5 (2C), 34.9 (2C), 43.8, 44.6 (2C), 50.9 (2C), 119.0, 121.4, 128.7, 130.8, 133.1, 135.8, 157.7, 158.5; HRMS (ESI), $m/z$ calcd for $C_{17}H_{22}Cl_2N_3O_2$ ($MH^-$) 370.1095, found 370.1105.

#### 4.1.9. $N^1$-(4-Chloro-3-methylphenyl)-$N^2$-(2,2,6,6-tetramethylpiperidin-4-yl)oxalamide (8c)

By use of a procedure similar to that described for the preparation of compound **8a**, the compound **6c** (482.0 mg, 2.00 mmol) was converted into the title compound **8c** (364.0 mg, 49% yield) as white powder.

$^1$H NMR (500 MHz, $CDCl_3$) $\delta$ 1.07 (t, $J$ = 12.0 Hz, 2H), 1.15 (s, 6H), 1.28 (s, 6H), 1.86–1.94 (m, 2H), 4.15–4.31 (m, 1H), 7.21–7.24 (m, 1H), 7.32–7.38 (m, 2H), 7.74 (s, 1H), 9.24 (s, 1H); $^{13}$C NMR (125 MHz, $CDCl_3$) $\delta$ 19.6, 28.5 (2C), 34.9 (2C), 43.7, 44.7 (2C), 50.9 (2C), 117.9, 120.2, 131.2, 133.1, 134.7, 135.1, 157.5, 158.8; HRMS (ESI), $m/z$ calcd for $C_{18}H_{25}ClN_3O_2$ ($MH^-$) 350.1641, found 350.1656.

#### 4.1.10. $N^1$-(3-Fluoro-4-methylphenyl)-$N^2$-(2,2,6,6-tetramethylpiperidin-4-yl)oxalamide (9a)

By use of a procedure similar to that described for the preparation of compound **8a**, the compound **7a** (225.0 mg, 1.00 mmol) was converted into the title compound **9a** (161.0 mg, 48% yield) as white powder.

$^1$H NMR (500 MHz, $CDCl_3$) $\delta$ 1.07 (t, $J$ = 12.5 Hz, 2H), 1.15 (s, 6H), 1.28 (s, 6H), 1.92 (dd, $J$ = 12.5, 3.50 Hz, 2H), 2.26 (s, 3H), 4.12–4.32 (m, 1H), 7.12–7.20 (m, 2H), 7.30–7.37 (m, 1H), 7.48–7.54 (m, 1H), 9.27 (s, 1H); $^{13}$C NMR (125 MHz, $CDCl_3$) $\delta$ 14.2, 28.5 (2C), 34.9 (2C), 43.7, 44.7 (2C), 50.9 (2C), 107.1 (d, $J$ = 26.3 Hz), 115.0, 121.8 (d, $J$ = 17.5 Hz) 131.6, 135.4, (d, $J$ = 15.0 Hz), 157.5, 158.8, 161.1 (d, $J$ = 242.5 Hz); HRMS (ESI), $m/z$ calcd for $C_{18}H_{25}FN_3O_2$ ($MH^-$) 334.1936, found 334.1942.

#### 4.1.11. $N^1$-(3-Chloro-4-methylphenyl)-$N^2$-(2,2,6,6-tetramethylpiperidin-4-yl)oxalamide (9b)

By use of a procedure similar to that described for the preparation of compound **8a**, the compound **7b** (482.0 mg, 1.00 mmol) was converted into the title compound **9b** (448.0 mg, 48% yield) as white powder.

$^1$H NMR (500 MHz, $CDCl_3$) $\delta$ 1.09 (t, $J$ = 12.5 Hz, 3H), 1.18 (s, 6H), 1.30 (s, 6H), 1.93–1.95 (m, 2H), 2.41 (s, 3H), 4.20–4.34 (m, 1H), 7.30–7.37 (m, 2H), 7.44–7.46 (m, 1H), 7.53 (d, $J$ = 2.50 Hz, 1H), 9.25 (s, 1H); $^{13}$C NMR (125 MHz, $CDCl_3$) $\delta$ 20.3, 28.5 (2C), 34.9 (2C), 43.7, 44.7 (2C), 50.9 (2C), 118.5, 122.0, 130.0, 130.7, 134.8, 137.1, 157.5, 158.8; HRMS (ESI), $m/z$ calcd for $C_{18}H_{25}ClN_3O_2$ ($MH^-$) 350.1641, found 350.1636.

#### 4.1.12. $N^1$-(3-Bromo-4-methylphenyl)-$N^2$-(2,2,6,6-tetramethylpiperidin-4-yl)oxalamide (9c)

By use of a procedure similar to that described for the preparation of compound **8a**, the compound **7c** (285.0 mg, 1.00 mmol) was converted into the title compound **9c** (157.0 mg, 40% yield) as white powder.

$^1$H NMR (500 MHz, $CDCl_3$) $\delta$ 1.07 (t, $J$ = 12.5 Hz, 3H), 1.15 (s, 6H), 1.28 (s, 6H), 1.91 (dd, $J$ = 8.00, 4.00 Hz, 2H), 2.38 (s, 3H), 3.70–3.75 (m, 1H), 7.22 (d, $J$ = 8.50 Hz, 1H), 7.30–7.37 (m, 1H), 7.43–7.45 (m, 1H), 7.90 (d, $J$ = 2.50 Hz, 1H), 9.25 (s, 1H); $^{13}$C NMR (125 MHz, $CDCl_3$) $\delta$ 22.4, 28.5 (2C), 34.9 (2C), 43.7, 44.7 (2C), 50.9 (2C), 118.6, 123.4, 125.0, 131.0, 134.9 (2C), 157.5, 158.8; HRMS (ESI), $m/z$ calcd for $C_{18}H_{25}BrN_3O_2$ ($MH^-$) 394.1136, found 394.1158.

#### 4.1.13. Amine (12)

The compound **11** was prepared according to the reported procedure.[14] To a stirred solution of piridone **11** (247.8 mg, 1.05 mmol) in MeOH (2.10 mL) was added *p*-methoxybenzylamine (0.41 mL, 3.15 mmol). After being stirred at room temperature for 23 h, sodium cyanoborohydride was added and stirred at room temperature for 48 h. The reaction mixture was poured into saturated $NaHCO_3$ and extracted with EtOAc, then dried over $MgSO_4$. After concentration under reduced pressure, the residue was treated with 1 M TMS in THF (4.8 mL). The mixture was stirred at 0 °C for 14 h. Concentration under reduced pressure followed by short chromatography with $CHCl_3$/MeOH gave the PMB-protected amine. To a solution of the above amine (584.0 mg, 1.64 mmol) in $CH_3CN/H_2O$ (13.1 mL, v:v = 2:1) was added CAN (2.74 g, 8.2 mmol). The mixture was stirred at room temperature for 14 h. The reaction mixture was diluted with 0.5 M HCl and washed with $CH_2Cl_2$. The water layer was alkalized and extracted with EtOAc, then dried over $Na_2SO_4$. Concentration under reduced pressure followed by flash chromatography over silica gel with EtOAc–EtOH (4:1) to gave the title compound **12** (175.5 mg, 71% yield) as a yellow oil.

$^1$H NMR (500 MHz, $CDCl_3$) $\delta$ 1.15–1.85 (m, 24H), 2.95–3.05 (m, 1H); $^{13}$C NMR (125 MHz, $CDCl_3$) $\delta$ 22.2 (2C), 22.8 (2C), 26.2 (2C), 37.3 (2C), 42.3 (2C), 43.6 (2C), 47.0, 53.2 (2C); HRMS (ESI), $m/z$ calcd for $C_{15}H_{29}N_2$ ($MH^+$) 237.2325, found 237.2321.

#### 4.1.14. $N^1$-((4-Chloro-3-fluorophenyl)-$N^2$-(2,6-dicyclohexylpiperidin-4-yl)oxalamide (13a)

By use of a procedure similar to that described for the preparation of compound **8a**, the compound **6a** (36.8 mg, 0.150 mmol) was converted into the title compound **13a** (7.6 mg, 12% yield) as yellow powder.

$^1$H NMR (400 MHz, $CDCl_3$) $\delta$ 0.71–2.28 (m, 24H), 2.03–2.20 (m, 2H), 4.02–4.16 (m, 1H), 7.13–7.18 (m, 1H), 7.27–7.33 (m, 1H), 7.62–7.66 (m, 1H), 9.25 (br, 1H); $^{13}$C NMR (125 MHz, $CDCl_3$) $\delta$ 14.1, 22.0 (2C), 22.6 (2C), 25.8 (2C), 29.3, 29.7 (2C), 31.9, 70.5, 108.3 (d, $J$ = 26.3 Hz), 115.8, 117.1 (d, $J$ = 18.8 Hz), 130.8, 136.2 (d, $J$ = 10.0 Hz), 157.6, 158.1 (d, $J$ = 247.5 Hz), 158.6; HRMS (ESI), $m/z$ calcd for $C_{23}H_{32}ClFN_3O_2$ ($MH^+$) 436.2162, found 436.2156.

#### 4.1.15. $N^1$-(4-Chlorophenyl)-$N^2$-(2,6-dicyclohexylpiperidin-4-yl)oxalamide (13b)

By use of a procedure similar to that described for the preparation of compound **8a**, the compound **6b** (31.3 mg, 0.120 mmol) was converted into the title compound **13b** (28.0 mg, 52% yield) as white powder.

$^1$H NMR (400 MHz, $CDCl_3$) $\delta$ 0.96 (t, $J$ = 12.5 Hz, 2H), 1.10–1.84 (br, 20H), 2.05–2.19 (m, 2H), 4.08–4.21 (m, 1H), 7.23–7.33 (br, 1H), 7.39–7.46 (m, 2H), 7.88 (t, $J$ = 1.00 Hz, 1H), 9.34 (s, 1H); $^{13}$C NMR (125 MHz, $CDCl_3$) $\delta$ 14.1, 22.1 (2C), 22.7 (2C), 26.1 (2C), 31.6, 37.2 (2C), 42.6, 43.0, 43.6, 52.6 (2C), 119.0, 121.4, 128.7, 130.8, 133.1, 135.8, 157.7, 158.5; HRMS (ESI), $m/z$ calcd for $C_{23}H_{32}Cl_2N_3O_2$ ($MH^+$) 452.1872, found 452.1865.

#### 4.1.16. $N^1$-((4-Chloro-3-methylphenyl)-$N^2$-(2,6-dicyclohexylpiperidin-4-yl)oxalamide (13c)

By use of a procedure similar to that described for the preparation of compound **8a**, the compound **6c** (121.0 mg, 0.500 mmol) was converted into the title compound **13c** (15.1 mg, 7% yield) as white powder.

$^1$H NMR (500 MHz, $CDCl_3$) $\delta$ 0.87–1.88 (br, 22H), 2.09–2.20 (m, 2H), 2.38 (s, 3H), 4.09–4.22 (m, 1H), 7.32–7.33 (m, 1H), 7.41–7.43 (m, 1H), 7.51 (d, $J$ = 2.00 Hz, 1H), 7.73 (m, 1H), 9.24 (s, 1H); $^{13}$C NMR (125 MHz, $CDCl_3$) $\delta$ 20.2, 22.1 (2C), 22.7 (2C), 26.0 (2C), 29.7, 37.0, 42.3 (2C), 42.8 (2C), 43.4, 52.9 (2C), 118.4, 122.0, 130.0, 130.6, 134.8, 137.1, 157.5, 158.9; HRMS (ESI), $m/z$ calcd for $C_{24}H_{35}ClN_3O_2$ ($MH^+$) 430.2267, found 430.2264.

#### 4.1.17. $N^1$-(3-Fluoro-4-methylphenyl)-$N^2$-(2,6-dicyclohexylpiperidin-4-yl)oxalamide (14a)

By use of a procedure similar to that described for the preparation of compound **8a**, the compound **7a** (225.0 mg, 1.00 mmol) was converted into the title compound **14a** (27.5 mg, 7% yield) as white powder.

$^1$H NMR (500 MHz, $CDCl_3$) $\delta$ 0.971 (t, $J$ = 12.5 Hz, 2H), 1.18–1.86 (m, 20H), 2.13–2.16 (m, 2H), 2.26 (s, 3H), 4.09–4.21 (m, 1H), 7.13–7.18 (m, 2H), 7.33 (d, $J$ = 8.00 Hz, 1H), 7.50–7.53 (m, 1H), 9.27 (s, 1H); $^{13}$C NMR (125 MHz, $CDCl_3$) $\delta$ 14.2, 22.2 (2C), 22.8 (2C), 26.1 (2C), 37.2 (2C), 42.2 (2C), 43.3 (2C), 43.5, 52.6 (m, 2C), 107.0 (d, $J$ = 27.5 Hz), 115.0 (d, $J$ = 3.75 Hz), 121.8 (d, $J$ = 17.5 Hz), 131.6 (d, $J$ = 6.25 Hz), 135.4 (d, $J$ = 10.0 Hz), 157.5, 158.9, 161.3 (d, $J$ = 242.5 Hz); HRMS (ESI), $m/z$ calcd for $C_{24}H_{33}FN_3O_2$ ($MH^-$) 414.2554, found 414.2562.

#### 4.1.18. $N^1$-(3-Chloro-4-methylphenyl)-$N^2$-(2,6-dicyclohexylpiperidin-4-yl)oxalamide (14b)

By use of a procedure similar to that described for the preparation of compound **8a**, the compound **7b** (120.5 mg, 0.500 mmol) was converted into the title compound **14b** (12.9 mg, 6% yield) as white powder.

$^1$H NMR (500 MHz, $CDCl_3$) $\delta$ 0.973 (t, $J$ = 12.5 Hz, 2H), 1.18–1.86 (br, 20H), 2.11–2.19 (m, 2H), 2.35 (s, 3H), 4.09–4.21 (m, 1H), 7.20–7.22 (m, 1H), 7.30–7.32 (m, 1H), 7.35–7.37 (d, $J$ = 2.50 Hz, 1H), 7.73 (m, 1H), 9.22 (s, 1H); $^{13}$C NMR (125 MHz, $CDCl_3$) $\delta$ 19.6, 22.1 (2C), 22.7 (2C), 26.0 (2C), 29.7, 37.0, 42.1 (2C), 42.7 (2C), 43.2, 53.3 (2C), 118.0, 120.3, 131.2, 133.0, 134.7, 135.1, 157.5, 158.8; HRMS (ESI), $m/z$ calcd for $C_{24}H_{33}ClN_3O_2$ ($MH^+$) 430.2267, found 430.2257.

#### 4.1.19. $N^1$-(3-Bromo-4-methylphenyl)-$N^2$-(2,6-dicyclohexylpiperidin-4-yl)oxalamide (14c)

By use of a procedure similar to that described for the preparation of compound **8a**, the compound **7c** (142.0 mg, 0.500 mmol) was converted into the title compound **14c** (11.5 mg, 5% yield) as white powder.

$^1$H NMR (500 MHz, $CDCl_3$) $\delta$ 0.67–2.07 (br, 22H), 2.28 (br, 2H), 2.38 (s, 3H), 4.09–4.21 (m, 1H), 7.22 (d, $J$ = 8.00 Hz, 1H), 7.28–7.38 (br, 1H), 7.43 (dd, $J$ = 4.50, 2.50 Hz, 1H), 7.90 (d, $J$ = 2.50 Hz, 1H), 9.21 (s, 1H); $^{13}$C NMR (125 MHz, $CDCl_3$) $\delta$ 14.1, 22.1 (2C), 22.4 (2C), 22.7 (2C), 25.9, 30.0, 31.6, 36.9 (2C), 42.7 (3C), 52.7, 52.9, 118.6, 123.4, 125.0, 131.0, 134.9, 135.1, 157.4, 158.8; HRMS (ESI), $m/z$ calcd for $C_{24}H_{33}BrN_3O_2$ ($MH^+$) 474.1762, found 474.1746.

### 4.2. Antiviral assay and cytotoxicity assay

Anti-HIV activity and cytotoxicity measurements in PM1/CCR5 cells (Yoshimura et al., 2010) were based on viability of cells that

had been infected or not infected with 100 TCID50 of an R5 primary isolate YTA48P exposed to various concentrations of the test compound. After the PM1/CCR5 cells were incubated at 37 °C for 7 days. The 50% inhibitory concentration ($IC_{50}$) values and the 50% cytotoxic concentration ($CC_{50}$) were then determined using the Cell Counting Kit-8 assay (Dojindo Laboratories). All assays were performed in duplicate or triplicate.

### 4.3. FACS analysis

JR-FL (R5, Sub B) chronically infected PM1 cells were pre-incubated with 0.5 μg/mL of sCD4 or 100 μM of a CD4 mimic for 15 min, and then incubated with an anti-HIV-1 mAb, 4C11, at 4 °C for 15 min. The cells were washed with PBS, and fluorescein isothiocyanate (FITC)-conjugated mouse anti-human IgG antibody was used for antibody-staining. Flow cytometry data for the binding of 4C11 (green lines) to the Env-expressing cell surface in the presence of a CD4 mimic are shown among gated PM1 cells along with a control antibody (anti-human CD19: black lines). Data are representative of the results from a minimum of two independent experiments. The number at the bottom of each graph shows the mean fluorescence intensity (MFI) of the antibody 4C11.

### 4.4. Molecular modeling

Dockings of compounds **3** and **13a** were performed using Molecular Operating Environment modeling package (MOE 2008. 10, Canada), into the crystal structure of gp120 (PDB, entry 3TGS).

## Acknowledgements

This work was supported in part by Grant-in-Aid for Scientific Research from the Ministry of Education, Culture, Sports, Science, and Technology of Japan, and Health and Labour Sciences Research Grants from Japanese Ministry of Health, Labor, and Welfare. We are grateful to Professor Yoshio Hayashi and Dr. Fumika Yakushiji, Tokyo University of Pharmacy and Life Sciences for their assistance in the molecular modelings.

## Supplementary data

Supplementary data (NMR charts of compounds) associated with this article can be found, in the online version, at http://dx.doi.org/10.1016/j.bmc.2013.02.041.

## References and notes

1. Chan, D. C.; Kim, P. S. *Cell* **1998**, *93*, 681.
2. (a) Kadow, J.; Wang, H.-G.; Lin, P.-F. *Curr. Opin. Investig. Dugs* **2006**, *7*, 721; (b) Repik, A.; Clapham, P. R. *Structure* **2008**, *16*, 1603.
3. Holz-Smith, S.; Sun, I. C.; Jin, L.; Matthews, T. J.; Lee, K. H.; Chen, C. H. *Antimicrob. Agents Chemother.* **2001**, *45*, 60.
4. Lin, P.-F.; Blair, W.; Wang, T.; Spicer, T.; Guo, Q.; Zhou, N.; Gong, Y.-F.; Wang, H.-F. H.; Rose, R.; Yamanaka, G.; Robinson, B.; Li, C.-B.; Fridell, R.; Deminie, C.; Demers, G.; Yang, Z.; Zadjura, L.; Meanwell, N.; Colonno, R. *Proc. Natl. Acad. Sci. U.S.A.* **2003**, *100*, 11013.
5. Zhao, Q.; Ma, L.; Jiang, S.; Lu, H.; Liu, S.; He, Y.; Strick, N.; Neamati, N.; Debnath, A. K. *Virology* **2005**, *339*, 213.
6. (a) Madani, N.; Schön, A.; Princiotto, A. M.; LaLonde, J. M.; Courter, J. R.; Soeta, T.; Ng, D.; Wang, L.; Brower, E. T.; Xiang, S.-H.; Do Kwon, Y.; Huang, C.-C.; Wyatt, R.; Kwong, P. D.; Freire, E.; Smith, A. B., III; Sodroski, J. *Structure* **2008**, *16*, 1689; (b) LaLonde, J. M.; Elban, M. A.; Courter, J. R.; Sugawara, A.; Soeta, T.; Madani, N.; Princiotto, A. M.; Kwon, Y. D.; Kwong, P. D.; Schön, A.; Freire, E.; Sodroski, J.; Smith, A. B., III *Bioorg. Med. Chem. Lett.* **2011**, *20*, 354; (c) LaLonde, J. M.; Kwon, Y. D.; Jones, D. M.; Sun, A. W.; Courter, J. R.; Soeta, T.; Kobayashi, T.; Princiotto, A. M.; Wu, X.; Schön, A.; Freire, E.; Kwong, P. D.; Mascola, J. R.; Sodroski, J.; Madani, N.; Smith, A. B., III *J. Med. Chem.* **2012**, *55*, 4382.
7. Curreli, F.; Choudhury, S.; Pyatkin, I.; Zagorodnikov, V. P.; Bulay, A. K.; Altieri, A.; Kwon, Y. D.; Kwon, P. D.; Debnath, A. K. *J. Med. Chem.* **2012**, *55*, 4764.
8. (a) Yamada, Y.; Ochiai, C.; Yoshimura, K.; Tanaka, T.; Ohashi, N.; Narumi, T.; Nomura, W.; Harada, S.; Matsushita, S.; Tamamura, H. *Bioorg. Med. Chem. Lett.* **2010**, *20*, 354; (b) Narumi, T.; Ochiai, C.; Yoshimura, K.; Harada, S.; Tanaka, T.; Nomura, W.; Arai, H.; Ozaki, T.; Ohashi, N.; Matsushita, S.; Tamamura, H. *Bioorg. Med. Chem. Lett.* **2010**, *20*, 5853; (c) Narumi, T.; Arai, H.; Yoshimura, K.; Harada, S.; Nomura, W.; Matsushita, S.; Tamamura, H. *Bioorg. Med. Chem.* **2011**, *19*, 6735.
9. (a) Schön, A.; Madani, N.; Klein, J. C.; Hubicki, A.; Ng, D.; Yang, X.; Smith, A. B., III; Sodroski, J.; Freire, E. *Biochemistry* **2006**, *45*, 10973; (b) Schön, A.; Lam, S. Y.; Freire, E. *Future Med. Chem.* **2011**, *3*, 1129.
10. Yoshimura, K.; Harada, S.; Shibata, J.; Hatada, M.; Yamada, Y.; Ochiai, C.; Tamamura, H.; Matsushita, S. *J. Virol.* **2010**, *84*, 7558.
11. Kwon, Y. D.; Finzi, A.; Wu, X.; Dogo-Isonagie, C.; Lee, L. K.; Moore, L. R.; Schmidt, S. D.; Stuckey, J.; Yang, Y.; Zhou, T.; Zhu, J.; Vicic, D. A.; Debnath, A. K.; Shapiro, L.; Bewley, C. A.; Mascola, J. R.; Sodroski, J. G.; Kwong, P. D. *Proc. Natl. Acad. Sci. U.S.A.* **2012**, *109*, 5663.
12. (a) Kwong, P. D.; Wyatt, R.; Robinson, J.; Sweet, R. W.; Sodroski, J.; Hendrickson, W. A. *Nature* **1998**, *393*, 648; (b) Kwong, P. D.; Wyatt, R.; Mcajeed, S.; Robinson, J.; Sweet, R. W.; Sodroski, J.; Hendrickson, W. A. *Structure* **2000**, *8*, 1329.
13. McFarland, C.; Vicic, D. A.; Debnath, A. K. *Synthesis* **2006**, 807.
14. Sakai, K.; Yamada, K.; Yamasaki, T.; Kinoshita, Y.; Mito, F.; Utsumi, H. *Tetrahedron* **2010**, *66*, 2311.